# Modern Galveston Island and the Brazos River Delta as Reservoir Analogs

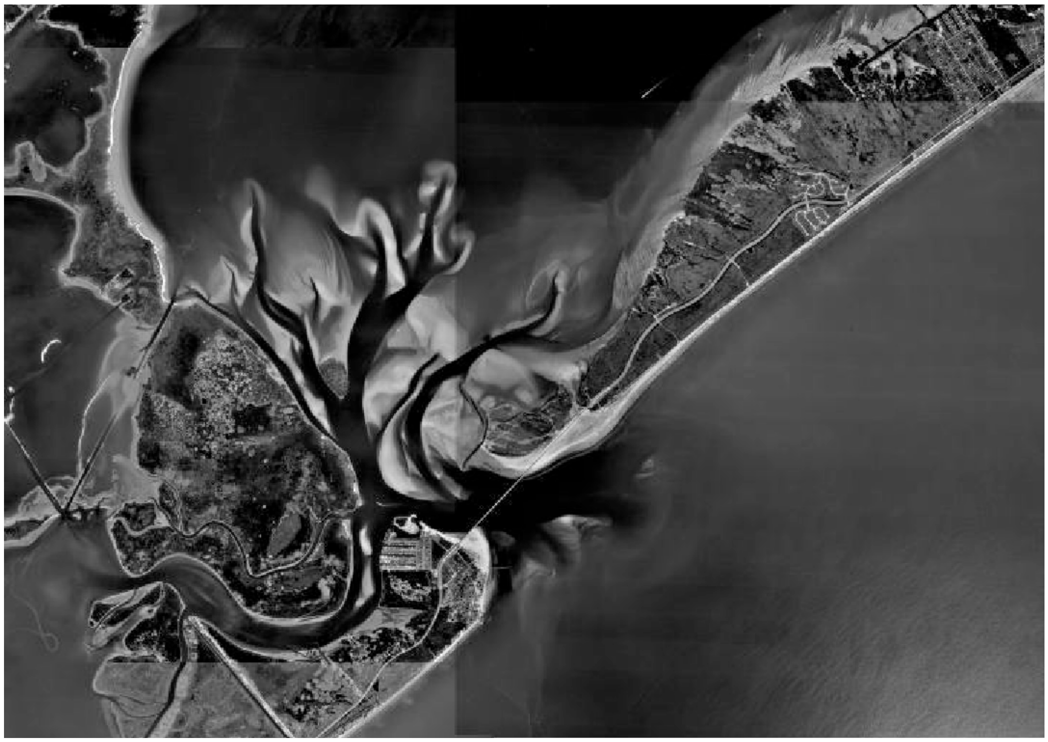

April 6th, 2017
SEPM Field Trip

Julia Smith Wellner
University of Houston
Department of Earth and Atmospheric Sciences

Davin J. Wallace
University of Southern Mississippi
Division of Marine Science

# Itinerary

**Depart at 8:00 am**
Take US 59 South to SH 288 South for ~15 miles
Turn Right on FM 1462

**Stop #1 The Brazos River Modern Point Bar**
Return to 521
Turn Right on 288 south to Angleton/Freeport
Take 36, towards Quintana Beach
Turn right on beach, drive to end

**Stop #2 New Brazos Delta and Beaches**
Return to Freeport, stop at gas station, drive to Surfside

**Stop #3 Old Brazos River Delta at Surfside Beach: Lunch**
*There may be bathrooms at this stop.*
Return to highway, head east toward Galveston Island
Just before bridge to Galveston, turn left at yellow bait shop

**Stop #4 Follets Island**
Return to highway, head east toward Galveston Island
Stop at Amigo Ln

**Stop #5 San Luis Pass**
*There may be bathrooms at this stop.*
Return to highway, cross toll bridge onto island
Stop at beach near Mile 16/Beach Access Point 18

**Stop #6 Galveston Island Beach**
Return to highway, head east
Turn right at slight hill

**Stop #7 Galveston Island Sea Wall End**
Return to highway and travel east to 61st Street (or drive through historic district if time to see houses that survived 1900 storm), Left on 61st Street to I-45 and return around 6:00 pm.

**Stop 1 - The Brazos River Modern Point Bar**

The rivers of east Texas (Sabine, Trinity, Brazos, Colorado, Lavaca rivers) vary significantly in terms of their sediment yields, which are in turn related mainly to the sizes of their drainage basins. These are all low gradient rivers that flow across extensive, virtually flat coastal plains and they have very broad flood plains where vast quantities of sediment are stored during highstands. Indeed, these alluvial valleys are currently filled virtually to capacity with sediments. Recently, the response of these rivers to climate and base-level change, in terms of sediment transport from the alluvial basins to the Gulf of Mexico, has been synthesized over the last 125 ka (Anderson et al., 2016) (Fig. 1). The sediment yields of these rivers today is significantly less than it was during most of the last eustatic cycle (Anderson et al., 2016). Today, the Brazos and Colorado rivers form small wave-dominated and bay-head deltas, respectively. During the previous highstand, both rivers nourished vast fluvial dominated deltas (Fig. 1). The fluvial channels of these ancestral rivers are preserved on the shelf and represent large reservoir-scale sand bodies within the highstand systems tract (Fig. 1).

During highstands, rivers meander broadly, resulting in wide meander belts with stacked channel/point bar/flood plain deposits. The fall in sea level was not continuous, but was rather punctuated by several prolonged pauses (Fig. 1). When sea level fall was rapid the river incised and when the rate of fall slowed the valley was widened to created terraces. This terraced morphology is common to all valleys that were active during the fall, except for smaller coastal plain rivers, such as the Lavaca and Calcasieu rivers.

During the lowstand that occurred between approximately 22 ka and 17 ka, the Brazos River incised to form a broad incised valley. This is the deepest incision and it corresponds to other deeply incised valleys on the shelf to form a prominent surface of relief, the sequence boundary (Fig. 1).

As sea level rose, this valley initially filled with fluvial sands filling the narrow portions of the valley (Fig. 1). As the transgression continued the broader portions of the valley were filled mostly with red flood plain clays that encase discrete fluvial channels. Aggradation of the valley shifted in an updip direction as the transgression continued.

During the relative still stand of the past 6,000 years the Brazos River occupied three channels, Big Sough, Oyster Creek and the modern channel (Figs. 2 & 3). These channels average 5 km in width, and are on average less than 15 m deep. Because they are so shallow, they are all being eroded as the shoreline advances landward via transgressive ravinement. The Colorado River occupied two channels, Caney Creek and the modern channel, during the late Holocene. Sand is confined to the basal portions of the Brazos channels, whereas the Colorado channels are mostly filled with sand.

Figure 4 illustrates the subenvironments of meandering rivers. The most sand-prone portion of the meandering river is the point bar. Lateral migration of meandering rivers results in lateral accretion of point bars and the development of extensive point bar deposits. Figure 5 shows an idealized point bar sequence and associated grain size distribution curves. Cut-and-fill structures and large-scale transport indicators (i.e., sand waves and troughs) dominate the basal channel deposit with clay rip-ups. The grain-size distributions of sands from the channel are coarse, poorly sorted, and negatively skewed. The lower point bar sequence includes a basal unit with giant ripple forsets and trough stratification. Sands within this part of the sequence are well-sorted (Fig. 5). The upper point bar is characterized by alternating parallel laminations and small ripples, indicating variable flow conditions during the waning stages of a flood. Sands of the upper point bar are finer and more poorly sorted than lower point bar sands (Fig. 5). They are fine skewed. Clay drapes separate individual flood deposits. As the river migrates laterally, point bar deposits are buried beneath fine sands, silts and clays of the natural levee and flood plain environments.

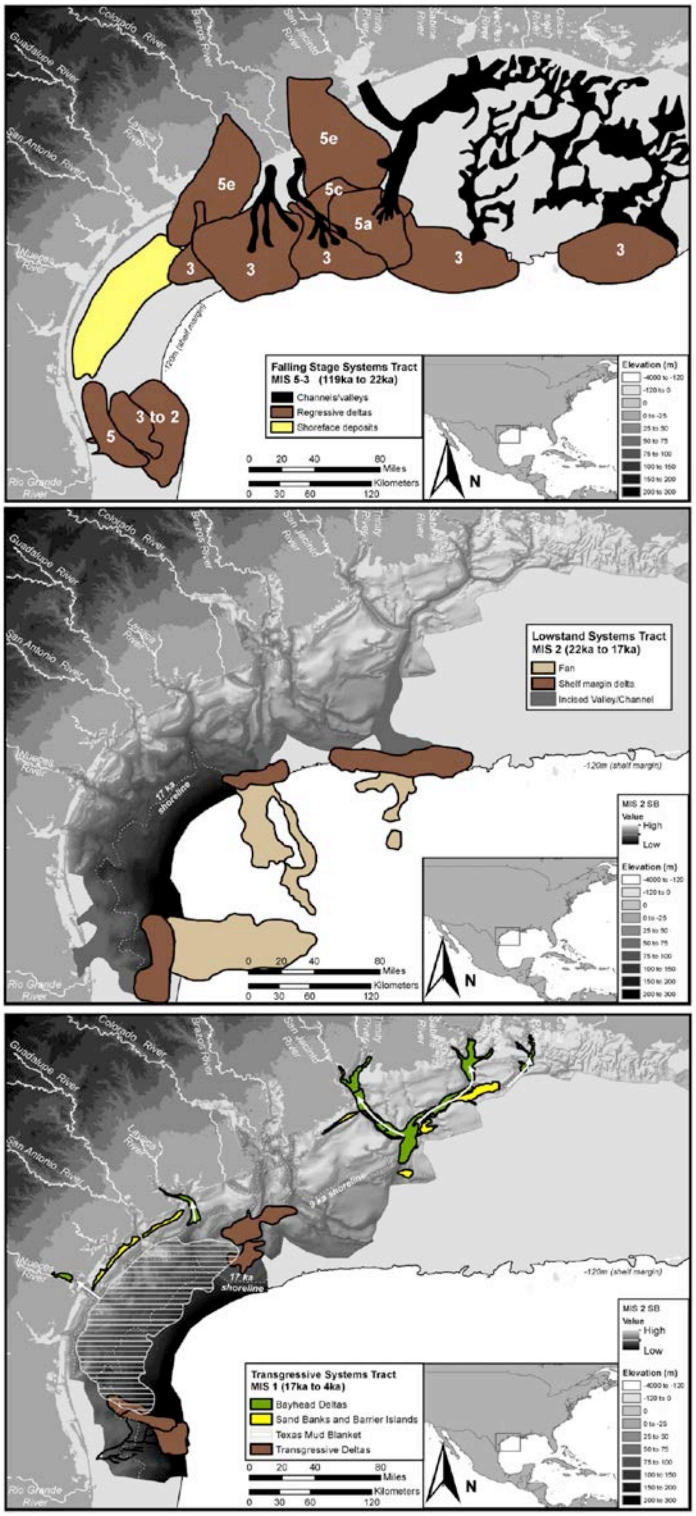


*Figure 1. (Top) Falling stage systems tract from 119 ka to 22 ka for the Texas coast. Note series of deltas from MIS 5e to 3 associated with the Colorado and Brazos Rivers (from Anderson et al., 2016, see references therein). (Middle) Digital elevation map of the Stage 2 sequence boundary showing major lowstand depositional systems between 22 ka to 17 ka for the Texas coast (from Anderson et al., 2016, see references therein). (Bottom) Transgressive systems from 17 ka to 4 ka for the Texas coast (from Anderson et al., 2016, see references therein). Note backstepping bayhead delta facies moving landward up the previous axis of the lowstand valleys.*

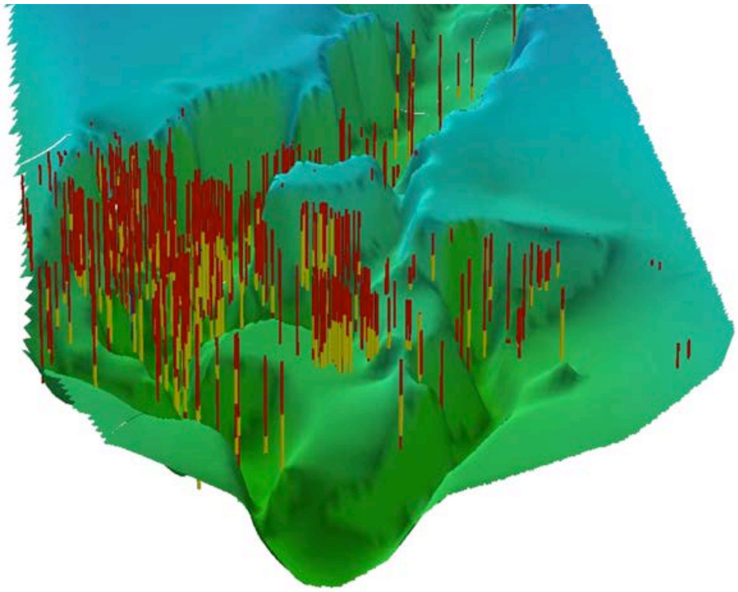

*Figure 2. Digital elevation map of the onshore portion of the Brazos valley showing locations of water wells that were used to map the valley and its fill. The yellow is sand and the red is clay. Work from Taha and Anderson, 2008.*

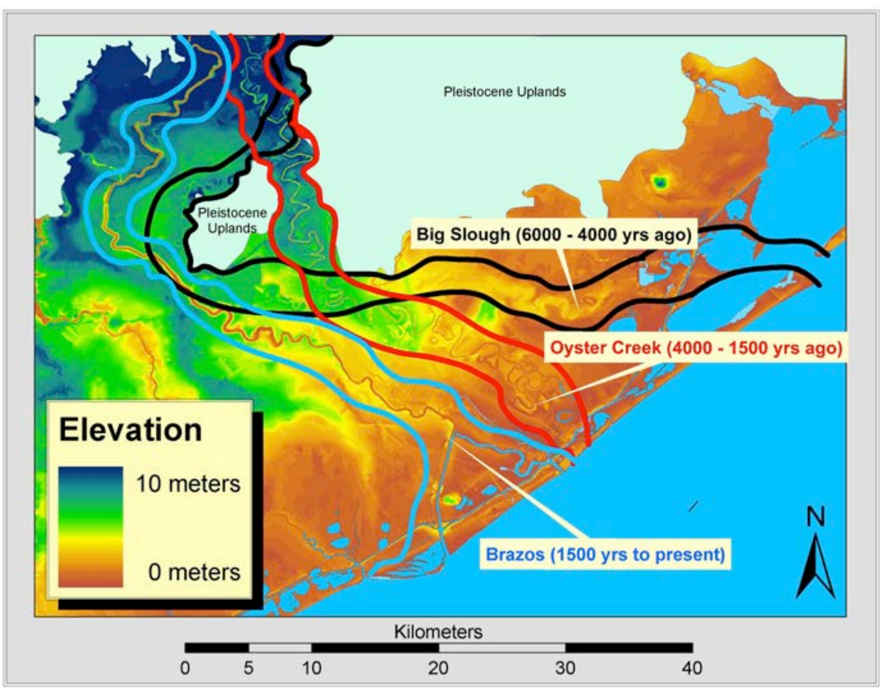


*Figure 3. Map showing the locations of the ancestral Brazos River channels that were occupied during the Holocene transgression. Work from Taha and Anderson, 2008.*

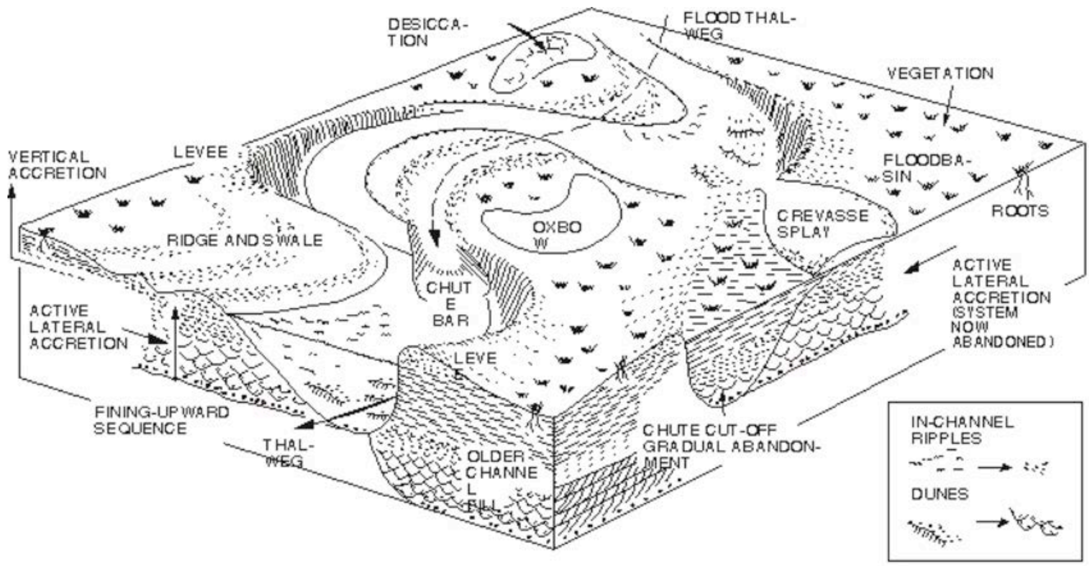


*Figure 4. Subenvironments and facies of a meandering river.*

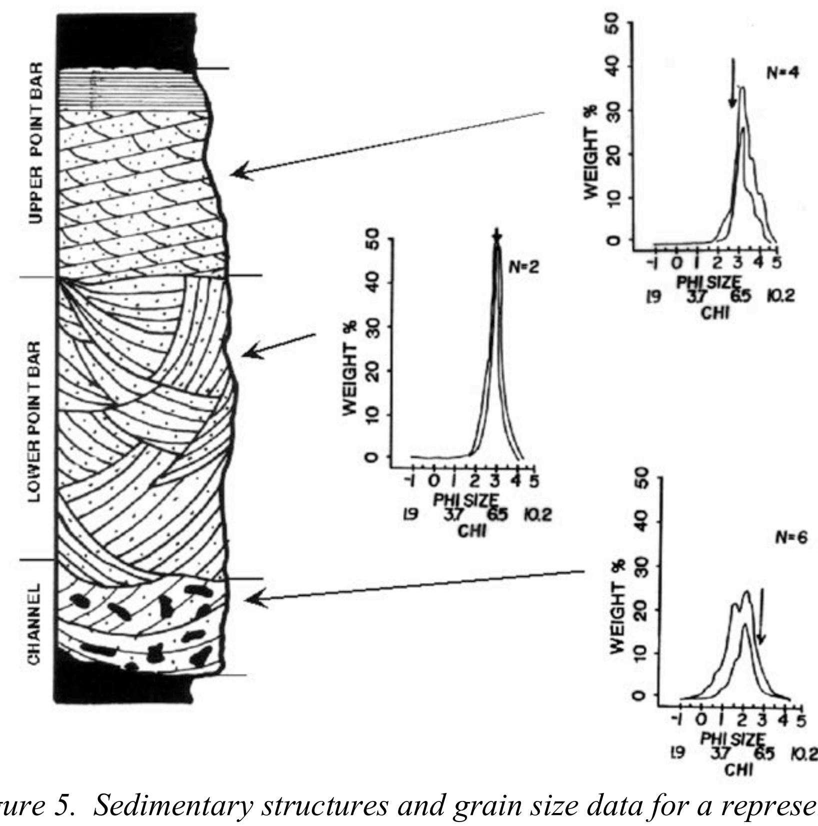


*Figure 5. Sedimentary structures and grain size data for a representative point bar deposit.*

The sequence illustrated in Figure 5 is an idealized one that would be formed by migration of the river channel in the absence of flooding. But, flooding results in an overall meandering river succession that consists of stacked, partial point bar deposits that together make up an overall fining upward sequence that is floored by channel deposits and capped by floodplain deposits. Bernard et al. (1970) acquired several long cores through a Brazos Point Bar succession near Richmond, Texas that shows this overall succession to be upwards of 18 m thick.

## Stop 2 - Brazos Delta

In 1929, the U.S. Corps of Engineers diverted the Brazos River mouth to its new channel west of Freeport. The present Brazos Delta, subsequently referred to as the new delta, was constructed and marine processes destroyed the old delta. The new delta is approximately 35 square kilometers in area and extends offshore to water depths of -20 meters (Fig. 6). The morphologic outline of the onshore deltas is lobate to lunate, with a significant headland on the western flank of the delta. Deposition is asymmetrical and accretes to the west along the projecting headland (Fig. 7).

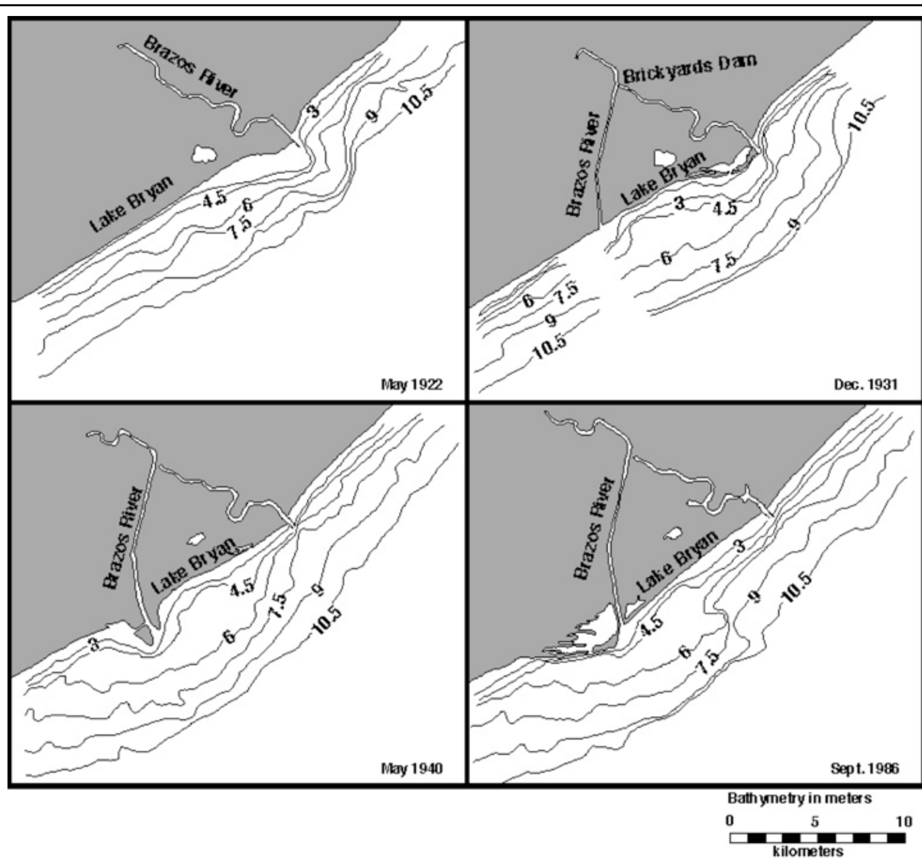


*Figure 6. Bathymetric maps constructed over several decades illustrate the changes in the offshore portions of the Brazos delta before and after the river's diversion in 1929. From Rodriguez et al., 2000.*

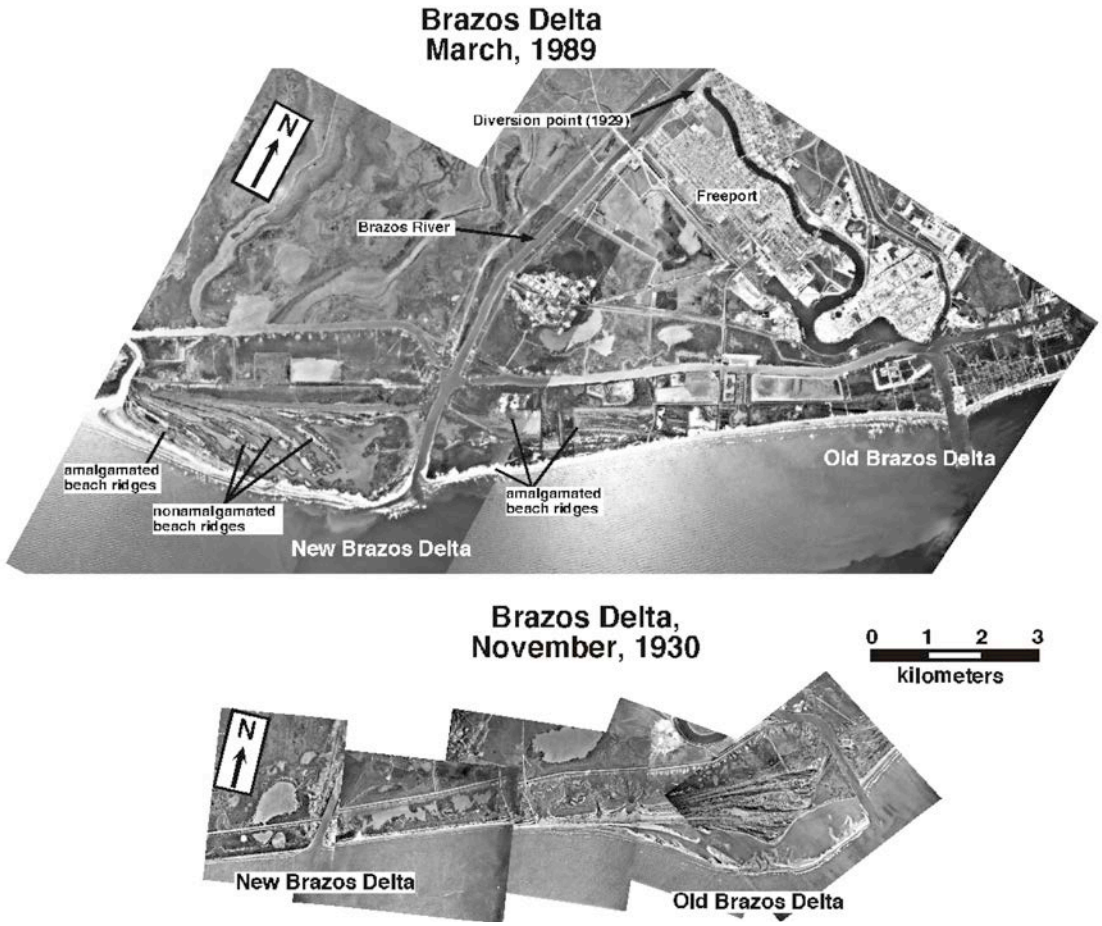


*Figure 7. Historical photographs showing changes in the Brazos delta after the river was diverted in 1929. From Rodriguez et al., 2000.*

The new Brazos delta is mostly situated above the level of shoreface ravinement, so it has little preservation potential during transgression. However, we know that during the last highstand, and during previous highstands throughout the Neogene, the Brazos River constructed sizable deltas on the continental shelf. Therefore, preservation potential of the delta is high during highstands.

Following diversion of the river in 1929, the delta experienced a rapid phase of growth that was due largely to sand being eroded from the pre-1929 delta and transported alongshore to the new delta. During this phase of growth, the Brazos delta was strongly wave-influenced and the facies architecture of the delta was comprised of well-sorted sand of stacked beach ridges (Bernard et al., 1970).

During December through February of 1992, the Brazos River experienced the most prolonged flood in historical time; the river was at flood stage for 80 days (Fig. 8). As a result of this event, sedimentation rates increased dramatically on both the onshore and offshore portions of the deltas. The Rodriguez et al. (2000) study led to the discovery that delta development has occurred in an episodic fashion, with episodes of dramatic growth being associated with major floods of this century (Fig. 9), followed by periods of wave reworking. Rice graduate student Carmen Fraticelli later argued (2006) that episodes of high sediment flux occurred during El Niño (wet) years that followed prolonged periods of dryness (La Niña years).

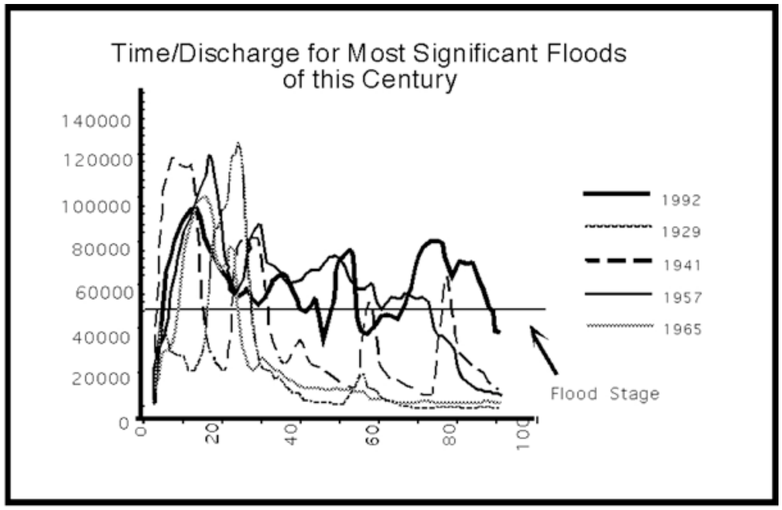


*Figure 8. Time versus discharge record for the Brazos River.*

During and immediately after the 1992 flood, field observations indicated that the regions closest to shore had experienced a net addition of sand, but nothing foretelling the emergence of a large offshore bar. Almost one year after the flood began, aerial photography showed the emergence of a bar approximately 1.9 km offshore (Fig. 9). One year prior to emergence, the bar zone was situated at 1 to 1.5 meters water depth. Gradually, the bar migrated onshore and alongshore, in an overall northwesterly direction, and eventually welded itself to the shoreline (Fig. 9).

Bar emergence created a second distinct depositional environment located landward of the bar classified as the back-bar lagoon. Because wave approach is generally from the southeast, sediment-laden river waters were deflected into this lagoon (with only a minor outlet at the west-end of the bar), rapidly filling it with fine-grained sediments. In the summer of 1992, the back bar was sufficiently deep (1.5 to 2.5 m) to allow coring operations from boats. By February 1993, the back bar aggraded to .5 to 1 m water depth. The sediments in this environment are silty clays with washover and eolian sands nearest the shorelines (Fig. 10).

Flood-associated deposition also occurred on the main shores of the delta, both east and west. Significant accumulation occurred on a headland of the west flank (Fig. 9). Spit accretion around this headland accelerated progradation of the shore locally. On the east flank of the delta, upper shoreface bars have recently become emergent and significant progradation of the eastern shore has occurred. Prior to the flood, the beach on the eastern shore was approximately 25 m wide. By February 1993, the beach had widened to nearly 100 m.

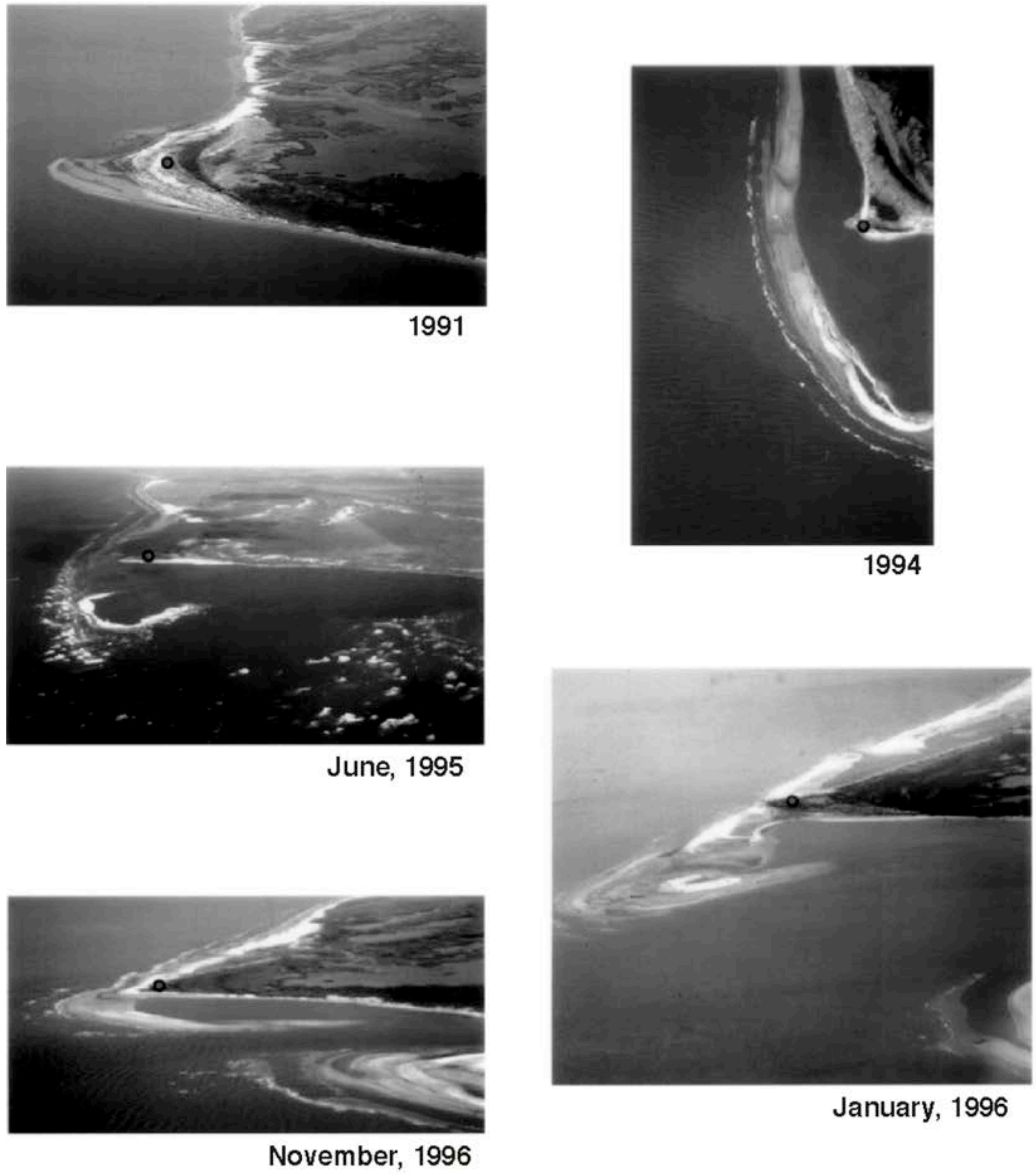


*Figure 9. Aerial photographs showing changes in morphology of the Brazos Delta prior to and after the 1992 flood. From Rodriguez et al., 2000.*

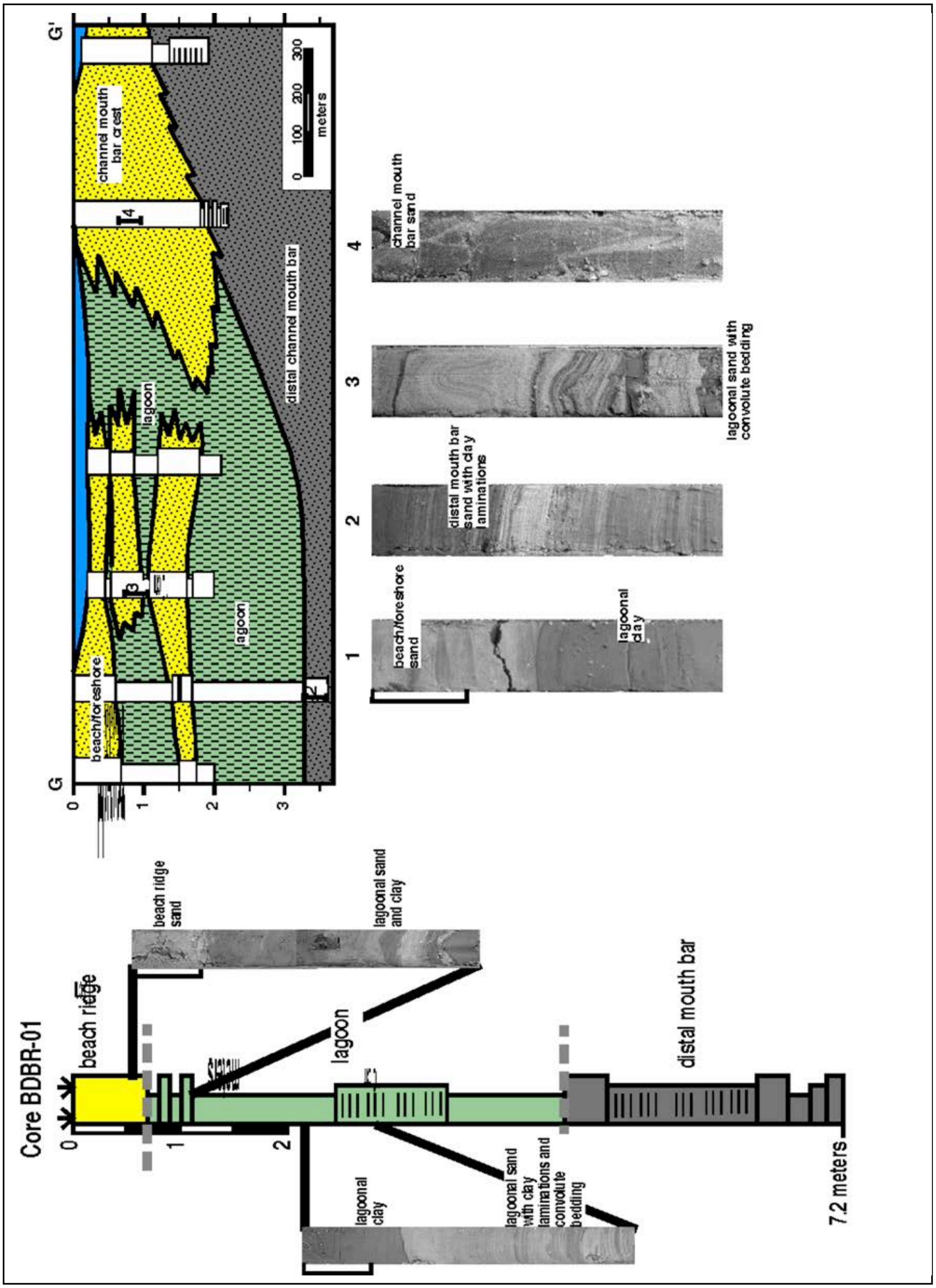


*Figure 10. Nearshore core transect across the Brazos Delta. From Rodriguez et al., 2000.*

During the flood, a tremendous amount of debris was brought to the delta. The river was nearly non-navigable due to the abundance of floating trees. This debris was accreted onto the shorelines, defining boundaries of flood-related accumulation. Each major flood results in a new debris zone on the shore. Successive floods can be identified from dates on the bottles and other garbage so that ridges can be correlated to the flood history shown in Figure 10.

**Prodelta**

A more recent study of the fine-grained material deposited in the pro-delta environment (Rice et al., in review) has shown the complexity of the inputs into this environment. This study used the same core collection as Rodriguez et al. (2000) but focused on detailed descriptions of the fine-grained material. 5 mud facies (Facies 1-5), as well as 4 sand and silt facies (Facies 6-9) were defined. The facies show significant differences in terms of grain size, thicknesses, lateral extent, and abundance in core, as well as stratigraphic characteristics in updrift and downdrift cores. Mud facies dominate the offshore region of the Brazos Delta, accounting for 64% of sediment downdrift and 89% of sediment updrift.

**Facies 1: Red Brazos Mud-**Facies 1 is pinkish-red mud (5 YR 4/3 on the Munsell Color Chart). Average grain size is 2.5-5 microns, while some samples (<25%) show peaks in the 6-8 micron range. X-ray diffraction shows predominantly illite, kaolinite, quartz, and calcite (Fig. 11). Organic matter is indicated by black-speckled "grains" throughout. Facies 5 always sharply overlies a browner or grayer mud facies and is typically found at the base of a mud package. This bottom contact is at times wavy, possibly due to scouring into underlying mud. Sand and silt beds are always found above this facies rather than within it. Bioturbation was not observed in facies 1. This facies is more abundant updrift than downdrift, as is evident from the distribution maps (Fig. 12). In downdrift areas, Facies 1 typically grades into a browner muddy facies. In the updrift region, similar gradations occur in cores near the river mouth and in cores closer to shore, however in cores farther updrift and offshore this facies is typically sharply overlain by thin Facies 4 (gray mud) interbeds. The red color and mineralogy, especially the abundance of calcite and illite, suggest the sediment originated in the Brazos drainage basin. This facies is considered to be the end-member Brazos provenance. The sharp lower contact suggests that it is primarily an early river flood deposit.

**Facies 2: Reddish-Brown Mixed Mud-**Facies 2 is reddish-brown mud (7.5 YR 4/2, Munsell Color Chart). Grain-size shows bimodal peaks at 2.5-5 and 10 microns. X-ray diffraction shows similar results to Facies 1 (illite, kaolinite, quartz, and calcite), but has a lower proportion of calcite. Also, a minor amount of smectite is present. Bioturbation is more common than Facies 1, however overall levels are still low (bioturbation indices of 0-1). This facies commonly shows a gradational contact with Facies 1 below, and it typically grades into Facies 3 above. Sand and silt streaks (<1 cm thick) are commonly found at the base or within this facies. This is the most abundant facies found throughout the Brazos Delta, both in terms of mud facies, as well as total sediment volume. The facies distribution map shows a dominance of this facies downdrift, and relative lack of abundance updrift (Fig. 12). Facies 2 is interpreted as primarily derived from the Brazos drainage, but the minor smectite, lower proportion of calcite, and the brown versus red color suggest some mixing with the updrift Mississippi provenance.

**Facies 3: Brown Mixed Mud-** Facies 3 is dark brown mud (10 YR 4/1, Munsell Color Chart). Grain-size shows a strong peak at 8-10 microns, and a smaller peak at 2.5-5 microns. X-ray diffraction identifies the main mineral constituents as illite, smectite, kaolinite, calcite, and quartz (Fig. 11). Very thin (<1 cm) sand and silt streaks are commonly found within this facies. This facies is typically found gradationally overlying Facies 2. It commonly grades into Facies 4 updrift, while downdrift it typically represents the uppermost facies in a mud package and is often sharply overlain by the redder mud facies of Facies 1 or 2. This facies is less common than Facies 2, and shows significant differences in abundance between updrift and downdrift cores (Fig. 12). The dark brown color, even amounts of smectite versus illiite, with some calcite suggests a mixed provenance mud, reflecting both Brazos and Mississippi sources.

**Facies 4: Grayish-brown Mixed Mud-**Facies 4 is a light gray mud that has a slightly brown tint (10 YR 4/2, Munsell Color Chart). The grain-size shows a strong peak at 8-12 microns, as well as a minor peak at 2-5 microns. X-ray diffraction identifies a stronger concentration of smectite and quartz than facies 1 to 3. Illite and kaolinite are also found, however samples showed no evidence of calcite (Fig. 11). Facies 4 is far more abundant updrift than downdrift (Fig. 12). In updrift cores, Facies 4 tends to occur as 1-3 cm thick interbeds, having sharp contacts above and below. Very thin brownish-yellow sand streaks were found in almost every occurrence. Downdrift, this facies did not occur as discrete interbeds, rather it typically had a gradational contact with Facies 3 below. Only in a few instances did this facies occur as interbeds downdrift of the Brazos River. The light gray color and dominance of smectite and quartz, as well as lack of calcite, suggest a predominantly Mississippi source. The slight brown tint suggest only trace amount of Brazos-derived mud

**Facies 5: Dark Gray Mississippi Mud**- Facies 5 is dark gray mud (5Y 3/2, Munsell Color Chart) with no brown tint. Grain size is similar to Facies 4, with a strong peak between 8-14 microns, and a smaller peak from 2-5 microns. X-ray diffraction shows this facies is composed of smectite, quartz, illite, kaolinite, and minor amounts of chlorite, indicative of continental shelf muds that are sourced from the Mississippi River. Unlike any other muddy facies, this facies is only found with sharp contacts above and below it, versus gradational contacts. Beds are typically less than 2 cm thick and occur mostly in the lower sections of cores taken in > 8 m water depth and in cores >10 km updrift from the Brazos River mouth. This muddy facies is nearly absent downdrift (<1% mud volume) and very rare updrift (<5% mud volume); it is only found in cores farthest updrift and in the lowermost portion of cores. The dark gray color and the mineralogy indicate an end-member Mississippi source. No mixing of Brazos source mud is indicated.

**Facies 6: Brownish-Yellow Very Fine Sand**-Facies 6 comprises brownish yellow, fine-grained sand. Grains appear to be 95% quartz, and are well rounded. Average grain size is 55-75 microns, with a small peak at 10 microns. In downdrift cores, sands often have discrete, wavy muddy lamina within them, which are likely responsible for the 10 micron-sized grains measured. This facies is predominantly found downdrift, but can be found updrift as well. Within downdrift cores, sand beds have average thicknesses of 7 cm, and can be up to 40 cm thick in water depths from 4-8 m. Updrift, beds are typically <5 cm thick and are generally found as thin streaks (<1 cm) farther offshore. Beds are most commonly found in the uppermost part of mud packages, typically within browner to grayer mud of Facies 2 to 4. They are almost never found at the base of a mud package that commences with a Facies 1 red mud. Downdrift, these sand beds are typically erosionally-based, scouring into what is typically brownish-red mud (Facies 2). The brownish yellow color and grain size suggest a Brazos provenance. Updrift sand may represent sand reworked from abandonment and erosion of the older pre-diversion Brazos delta

**Facies 7: Brazos-derived Orange Silt** Facies 7 comprises orange silt (7.5 yr 6/6, Munsell Chart) and is darker in color and finer-grained that facies 6. Typical grain sizes are 25-35 microns with a smaller peak at 3.5 microns. In cores taken in water depths less than 8 m, occurrences of this facies can be up to 20 cm thick downdrift, and 8 cm thick updrift of the Brazos River. Farther offshore it is expressed as streaks <1 cm thick, however, downdrift cores tend to have thicker beds offshore than in the updrift cores farther offshore. It is the most common non-muddy facies in downdrift cores. This facies is much more abundant downdrift than updrift. The orange color, thinning away from the river mouth, and predominance downdrift suggest a Brazos provenance.

**Facies 8: Orange-Brown Muddy Sand** Facies 8 comprises orange-brown muddy sand (Munsell 7.5 YR 5/6). Grain size of this facies shows a strong peak at 90 microns (very fine sand), with smaller peaks at both 13 and 3 microns. There are starved ripples within this facies composed of the previously discussed brownish-yellow sand of facies 7. This facies is found primarily in the center of the delta, accounting for 80% of sediment in core BD 93-01, but throughout the entire delta it is otherwise very rare (<5% sediment). It does not appear to have any distinguishable differences in updrift vs. downdrift environments, as it is localized near the river mouth. The orange color and proximity to the modern Brazos river mouth suggests that it is derived directly from the Brazos River.

**Facies 9: Brown Silty Mud** Facies 9 comprises brown silty mud (Munsell 7.5 YR 4/2). Grain size analysis shows bimodal peaks, at 18 microns and 3 microns respectively. Mud samples downdrift show decreasing amounts of the 18 micron peak farther away from the Brazos River mouth. Like the orange brown muddy sand (Facies 8), this facies is primarily found near the center of the delta, however it is more common downdrift than updrift. This facies is not found in any appreciable abundance in cores > 5 km from the river mouth downdrift, and is basically absent updrift. The proximity to the center of the delta suggests a primary Brazos origin. Silts are likely mixed with the muds of facies 1, 2 and 3 with decreased silt farther offshore.

**Mud Packages and Facies Successions:** The individual facies described above could in turn be grouped into distinct packages or beds (i.e., laminasets). Each package commonly shows a sharp-based layer of red mud (Facies 1 or 2), which grades up into a brownish mud (facies 3), and finally into a gray mud (facies 4 and 5) at the top. These packages are typically 2-10 cm thick, and define bed-scale features, which are internally heterolithic. These are interpreted as probable flood deposits, in which Brazos river-derived red mud (during flood) grades into longshore-derived gray mud. The mud packages can in turn be grouped into an overall facies succession. In general, most cores show an overall coarsening and thickening upwards of beds, which is consistent with an overall prograding deltaic system. Several cores (e.g., marked by a thick sand at about 90 cm in core BP 23) show a pair of coarsening upward bedsets, which implies several stages of progradation. There were significant and consistent differences of mud packages in terms of facies type and stratigraphic characteristics between the updrift and downdrift regions of the delta (Fig. 13).

Updrift muds are generally composed of 27% Facies 1 (red Brazos mud) and 30% of Facies 4 (gray/mixed mud) within the cored successions. Facies 2 and 3 represent the remaining 43%. Facies 1 and Facies 4 are more abundant in cores > 8 km offshore from the Brazos River mouth. Updrift mud packages also show distinctly sharper contacts between successive beds of facies 1 and 4, with less grading into browner muds, as is more common downdrift. This interbedded pattern is most common in cores farthest updrift, offshore, and in the lower portions of cores. Gradational transitions of red to gray mud were most common in cores near the river mouth and nearshore.

Sand and silt streaks were commonly found at the tops of mud packages within Facies 4. Thicker erosionally-based sands were present in the six updrift cores closest to the Brazos River mouth. In one offshore core (BDP 04) as many as 7 erosionally-based sands and silts were recorded, which overlay reddish Brazos mud deposits. Thin sand layers less than 20 cm could be correlated over 8 km offshore (Fig. 14).

Mud packages downdrift are dominated by the two mixed mud facies, and comprise 52% of Facies 2 and 27% of Facies 3 (Fig. 12). Facies 1 accounts for 14% of total mud volume, and Facies 4 accounts for only 6%. All mud in the downdrift region has a tint of brown, therefore Facies 5 (end-member Mississippi mud) is absent. Downdrift mud packages typically have subtle, gradational changes in facies type. Mud packages usually have a basal unit of Facies 2, which grades into Facies 3. This is then sharply overlain by the next mud package, which starts again with Facies 2. Orange silt beds are the most common non-muddy facies identified within downdrift mud packages. Multiple streaks could be found within single mud packages downdrift. Silt beds >3 cm thick were most commonly found above the base of mud packages, however they could also be found scouring into Facies 1 (~25% of beds).

The stratigraphic differences between the updrift and downdrift regions are clearly shown in the strike view cross-section (Fig. 15) and show three significant stratigraphic trends: 1) Sand and silt beds are far more abundant downdrift than updrift and they often occur within mud packages rather than at the base, 2) The two end member mud facies, Facies 1 and 4, are far more abundant updrift, whereas the mixed mud facies 2 and 3 dominate in the downdrift area, and 3) downdrift mud packages have gradational transitions from red to gray mud, while updrift mud packages tend to have sharp contacts between facies. The sand and silt facies are far more common downdrift than updrift. These coarse-grained facies typically occur 2-3 cm above the base of a muddy flood deposit (i.e. mud package) and often have erosional contacts. This is important because sand and silt layers are conventionally deemed the base of a flooding succession. This was not typical within these cores, especially farther offshore. When looking strictly at grain size within mud packages, the occurrence of these erosionally based sand and silt layers give the mud package an inverse to normal grading pattern. This inverse to normal grading is similar to the proposed hyperpycnite model of Mulder et al. (2003). Within a 100 cm core (representing less than 80 years of deposition), these intervals occurred as many as 6 times in a single core.

**Brazos River Hydrograph Data:** Hydrograph data, from the Richmond gauging station in Fort Bend County, Texas (USGS National Water Information System web interface, 2009), shows large variations in monthly discharge, that are fairly consistent every year. Average peak daily discharge of about 400 $m^3$/sec occurs in May. The lowest average daily discharge of about 80 $m^3$/sec occurs during August. These values reflect the wet and dry seasons in the Brazos drainage basin.

The duration of a Brazos River flood varies depending on the size of the flood. Floods < 300 $m^3$/sec tend to occur for less than 30 days and have one peak in discharge, while large floods > 600 $m^3$/sec can last several months and have several peaks during the duration of the flood. These larger floods have internal peaks and troughs in discharge as the river waxes and wanes during the flood's long-term duration.

**Oceanographic Data:** Daily longshore currents crossing the Brazos Delta were analyzed from 1993-2008. Longshore currents had variable intensities and directions, however for practical reasons longshore currents were recorded as either normal or reversed. Normal longshore currents had a southwesterly direction, while reversed currents had a northeasterly direction. Current direction was extremely variable along the Texas Gulf Coast, therefore values were recorded in terms of current direction crossing the Brazos River mouth.

From 1993-2008, longshore currents were normal 58% of the time and reversed 42% of the time. However, in 2001, 2003, and 2008 reversed longshore currents were actually more common. During this 16 year period, there were >100 changes in longshore drift (normal to reverse, or reverse to normal). The average consecutive days of normal longshore currents before a reversal was 26 days, while reversed longshore currents averaged 17 consecutive days before changing back to normal.

Specific longshore current direction shows trends during certain months in the year. There is a preference of normal currents during the Fall, Winter, and Spring months (September-May: 75% of days during this time), while the Summer months of June-August show a preference of reversed currents (70% of days during this time). The month with the highest probability of having normal longshore currents is May (90% normal), which also coincides with the periods of typically highest discharge. On the other hand, reversed currents dominate during July (85% reversed).

Longshore currents deflect river discharge to the southwest during normal longshore currents, and to the northeast during reversed currents. This has been shown in multiple aerial trips over the Brazos Delta. Since water discharge varies throughout the year, it is important to know when the direction of longshore currents are normal, and when they are reversed. Individual floods were analyzed from 1993-2008 and compared to the temporal longshore current directions operating at the time of the flood. Figure 16 shows significant discharge events from 1993-2008 in comparison to longshore current direction at the time of the flood. As the figures illustrate, there is no significant relationship between longshore current direction and major flood events. The chart indicates major floods occur during both normal and reversed longshore currents.

**Bathymetric Profiles:** Historical bathymetric maps show that the Old Brazos Delta had little to no bathymetric expression after 1940 (Rodriguez et al., 2000). This indicates erosion of the prodelta environment in water depths up to 10.5 m. Sediment deposited shallower than 10.5 m may be susceptible to fair-weather wave-reworking and erosion. This is significant when considering that sediment in the Old Brazos Delta was more compacted than the relatively less consolidated Modern Brazos deposits. When evaluating the bathymetric profile of the Brazos Delta today, the inner shelf of the downdrift region is broader, shallower, and has a much more gentle slope than the updrift region.

**Formative Processes and Interpretation:** Analysis of the initial and post-depositional history of a single Brazos River flood deposit exemplifies the processes likely responsible for the stratigraphic differences in the Brazos prodelta. In one set of cores, taken in January 1992 two weeks after the peak of a major flood, as much as 50 cm of sediment was found in the center of the delta, and slightly downdrift as well. This indicates rapid deposition, possibly from a hyperpycnal flow. Cores taken six months later in July showed a dramatic shift of these previous flood deposits, indicating reworking to the updrift side of the delta. As much as 60% (30 cm) of the initial deposit was redistributed updrift. The area of greatest remobilization occurred in areas with shallower water depths. Deeper areas showed less remobilization, probably because they are less susceptible to wave-induced resuspension of sediment and consequent redistribution to the updrift region.

**Wave-suspended Fluid Mud in the Brazos Delta:** It is proposed that post-depositional mobility of Brazos prodelta sediment is an important process responsible for the stratigraphic differences between updrift and downdrift muddy deposits. As a wave - influenced delta, with a relatively shallow prodelta, the Brazos Delta is likely susceptible to wave-induced resuspension and remobilization of unconsolidated muds. There are two indications that wave-induced resuspension is an active process. The first is the redistribution of the 1992 flood sediment. The second indication comes from aerial photos taken during the summer of 2009 when discharge was anomalously low (Fig. 17). Discharge had been anomalously low during the previous two months, however the Brazos Delta had a sediment-laden water column. The suspended sediment was not sourced directly from the Brazos River, as was evident from the relatively clear river plume. Rather, red mud from previously deposited flood sediment in the downdrift region was likely being transported updrift due to wave-induced resuspension.
As an asymmetric delta with bathymetric differences between the updrift and downdrift regions, it is unlikely that wave-induced resuspension and redistribution has an equal effect on both sides of the delta. As a result, the deposits within both regions of the delta (updrift and downdrift) differ.

**Offshore Bathymetric Differences in Wave Resuspension:** As seen in the bathymetric profile of the Brazos Delta (Fig. 18), there is a steep seabed slope starting 2 km updrift of the Brazos River mouth within the offshore region. Downdrift of the Brazos River, the increase in water depth is more gradual and the overall water depths are shallower. Because of these bathymetric differences, the downdrift region is expected to have a larger area, which falls above fair-weather wave base, than in the updrift region. However, the downdrift region is typically protected from waves during normal longshore current flow because of the groin effect from river discharge. During times of normal longshore currents, the updrift side is exposed to the full force of waves, but because the majority of the updrift region falls below fair-weather wave base, little or no sediment resuspension occurs during fair-weather conditions.

During reversed currents, river discharge is deflected to the northeast, which leaves the southwest region exposed to the full force of waves. The difference in the downdrift region is that the majority of the seabed falls above fair-weather wave base, and sediment in this region is thus more susceptible to wave-induced resuspension and remobilization than the deeper updrift area. It is hypothesized that wave-resuspension is primarily responsible for the mixed mud facies found downdrift, and the deeper water and consequently lower wave-energy updrift area lacks this evidence of mixing.

**Explanation for Sand and Silt Abundance Downdrift:** The abundance of the sand and silt Facies 7, 8, and 9 found downdrift are likely sourced from the Brazos River, which are then deflected downdrift due to the more commonly occurring southwestern longshore currents. These sand and silt beds are commonly found above the base of a flooding succession, indicating the red mud (Facies 1) is deposited first, possibly due to hyperpycnal conditions. The occurrence of Facies 6, the brownish-yellow sand, found both updrift and downdrift are likely tied to high-energy storm events. These sand streaks are commonly found within the gray Facies 4 mud, which supports the hypothesis that these gray muds are derived from high-energy events, and represent resuspended gray continental shelf mud.

In the nearshore region of asymmetric deltas the updrift region is often considered to be sandier than the downdrift region. In the offshore region, as indicated by this study, the opposite may be true where the downdrift region has more sand than the updrift region.

**Prodelta Depositional Model:** Times 1-6 in this model are separated by long-term changes in longshore current direction. While longshore currents may switch in a matter of days, this model is meant to indicate larger scale longshore current variations attributed to seasonal patterns (Fall-Spring = Normal Currents, Summer = Reversed), and high-energy events, such as storms, which often coincide with reversed longshore currents. Time 6, the final period, represents the onset of the next flood, and a new cycle.

On average, major floods have occurred every 2 years from 1929-2009. While this model represents the time from one major flood to the next, there are likely pulses of Brazos-derived sediment pertaining to minor flooding events throughout the time series. This model, however, considers one major influx of sediment in Time 1, a significant decrease in discharge by Time 3, and another major flood in Time 6. The complete model is shown in Figure 19 and provides a map view of the processes involved, a strike-view cross-section, and a depiction of facies and stratigraphy in an updrift and downdrift core.

Time 1 is designated as the period when the Brazos River is in flood. Red Brazos mud (Facies 1) is rapidly deposited in the center of the delta (possibly by hyperpycnal conditions), while additional suspended sediment is transported to the southwest. In this example, longshore currents are normal (flowing southwest), and the plume is partially deflected to the southwest. At this time, there is relatively less Brazos sediment distributed in the northeastern region.

Time 2 represents a time when discharge subsides, longshore currents are reversed, and flood sediment is remobilized to the northeast. With sediment and water discharge deflected updrift, waves are able to resuspend and redistribute flood sediment from the southwest region to the northeast. At this point, Facies 1 is likely the surficial sediment across the entire delta. Time 3A represents a time when Brazos River discharge has fallen significantly and longshore currents are normal again. During this time, sediment in the northeastern region is relatively stable as it lies below fair-weather wave base. In the southwest, there are two sources of sediment: 1) sediment derived directly from the Brazos River mouth, and 2) sediment initially deposited in the center of the delta, which is remobilized farther southwest.

Time 3B represents a continuance of normal longshore currents, and during this time, a pulse of longshore transport-derived gray mud is introduced to the delta, possibly related to a storm over the continental shelf. This gray mud sharply overlies the Facies 1 deposits in the northeast region. Nearshore in the northeast region, waves are likely to mix this gray mud with the underlying red mud, while farther offshore they are preserved as Facies 4 layers. Because of the hydraulic groin and a sediment-laden water column, this pulse of gray mud is less likely to infiltrate the southwest region in significant amounts. The majority of this gray mud is found farther offshore where these barriers are less significant. Any gray mud that does infiltrate the southwest region is likely mixed with the red mud from the Brazos River.

Time 4 represents another reversal in longshore currents. In the southwest, waves are able to resuspend surficial sediment and mix the two mud types (red and gray) deposited in the previous time series. This mixing results in brownish muds (Facies 2 and 3), which is the most abundant facies found in the southwest. The mixed muds are likely redistributed to the northeast as suspended sediment and/or a fluid mud, which sharply overlies the gray mud introduced in Time 3.

Time 5A represents normal longshore currents again. During this time, discharge and sediment coming from the Brazos River has dropped significantly, therefore the majority of the sediment delivered to the southwestern region is coming from remobilized surficial deposits in the center of the delta, which tend to be redder than the browner facies created during Time 4. In the northeast, the surficial mixed muds deposited during Time 4 are likely relatively stable offshore, as they lie below fair-weather wave base.

During Time 5B, normal longshore currents continue, and another pulse of gray mud crosses the delta. In the northeastern region, this gray mud sharply overlies the mixed muds farther offshore, while nearshore it is mixed with the previously mixed brownish muds. In the southwestern region, this gray mud partially mixes with the Brazos-derived mud sourced from the Brazos River.

This cycle continues until the next flooding event occurs. Time 6 represents the onset of the next flood, therefore it can be considered as the next Time 1 where the whole process starts over. The underlying mud package (deposits during Time 1-5) is sharply overlain by the next flood deposit (Facies 1).

Within this complete sequence, from one major flood to the next, there are often multiple sharp contacts of relatively redder mud overlying browner mud termed here as mud packages. It is proposed that these sharp contacts are not necessarily due to individual floods, rather they may represent the remobilization of wave-induced fluid muds. Although there are multiple sharp contacts within a single flood sequence, the fact that each mud package becomes progressively enriched in gray mud up core indicates these are not individual floods, rather they are the product of recycled sediment from the initial flood.

This model accounts for the two mud facies differences between the updrift (northeastern) and downdrift (southwestern) regions which were: 1) the abundance of Facies 1 and Facies 4 updrift, and dominance of the mixed facies downdrift, and 2) the sharp contacts between facies updrift, and the gradational contacts between facies downdrift. These differences are both related to the ability of waves to rework the downdrift region, while the updrift region is relatively stable, and also the greater supply of Brazos sediment downdrift due to the extended prodelta tail and the lack of a constant supply of Brazos-derived sediment updrift.

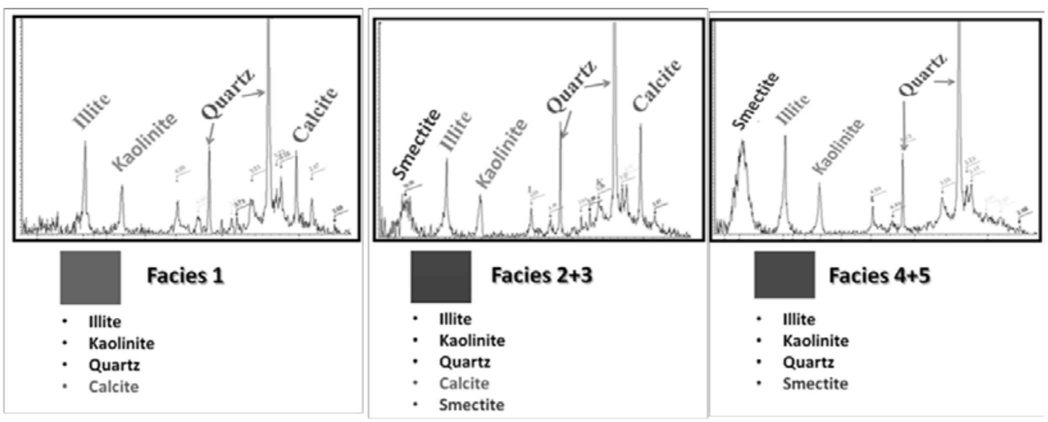


*Figure 11. XRD mineralogy results for each mud facies.*

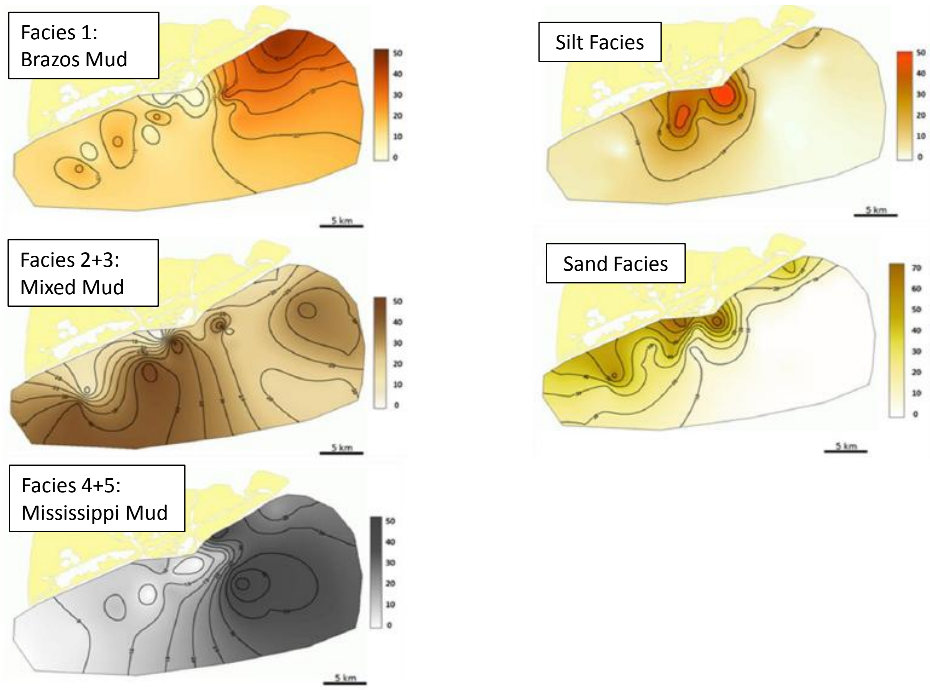


*Figure 12. These distribution maps show the trends of where these facies were most commonly found throughout the Brazos Delta. Muddy Facies (left) are plotted in % of total mud volume. Sand and silt facies (right) are plotted in % of total sediment volume. In terms of the muddy facies (left column), the updrift side is primarily composed of Facies 1, and Facies 4+5, the two end-members. The downdrift region is dominated by the mixed facies. The sand and silt facies both show similar trends, as they are the most abundant nearshore, and are clearly more abundant downdrift of the Brazos River.*

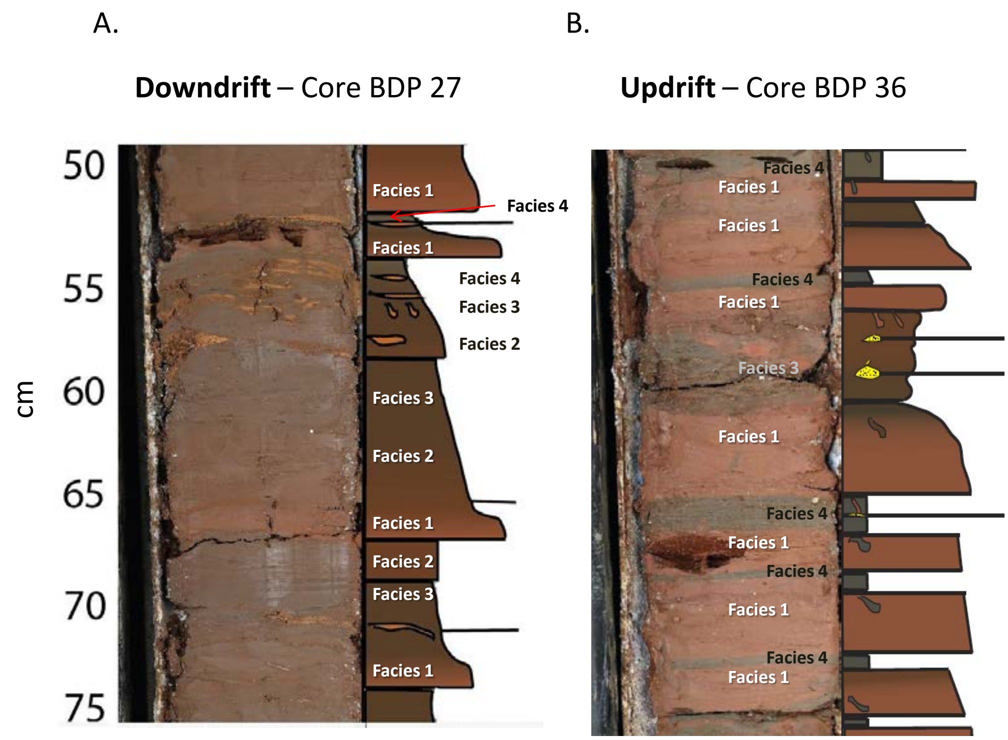


*Figure 13. Comparison of typical updrift vs. downdrift mud packages. A. Downdrift from core BDP 27. B. Updrift from core BDP 36.*

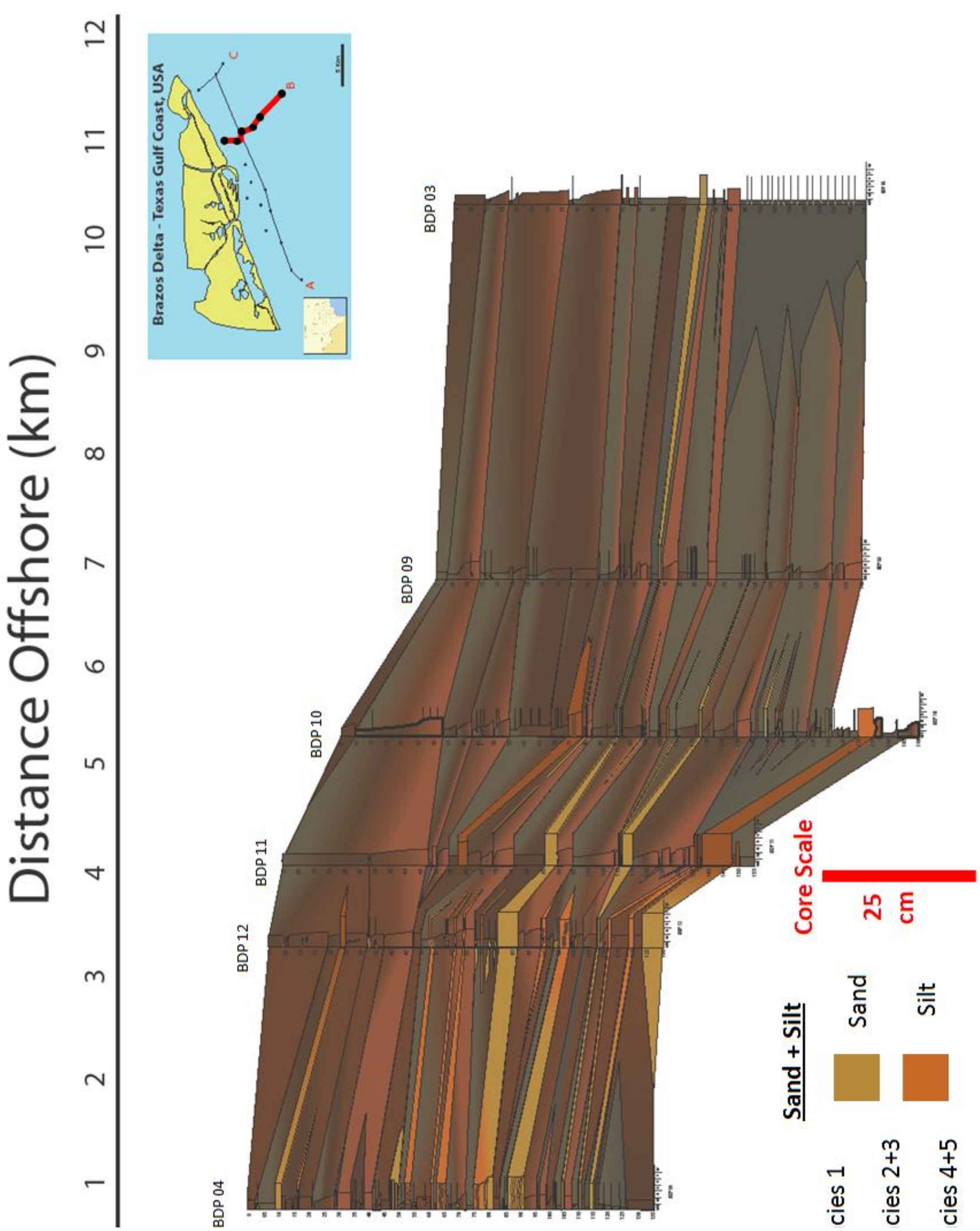


*Figure 14. Dip-oriented cross section.*

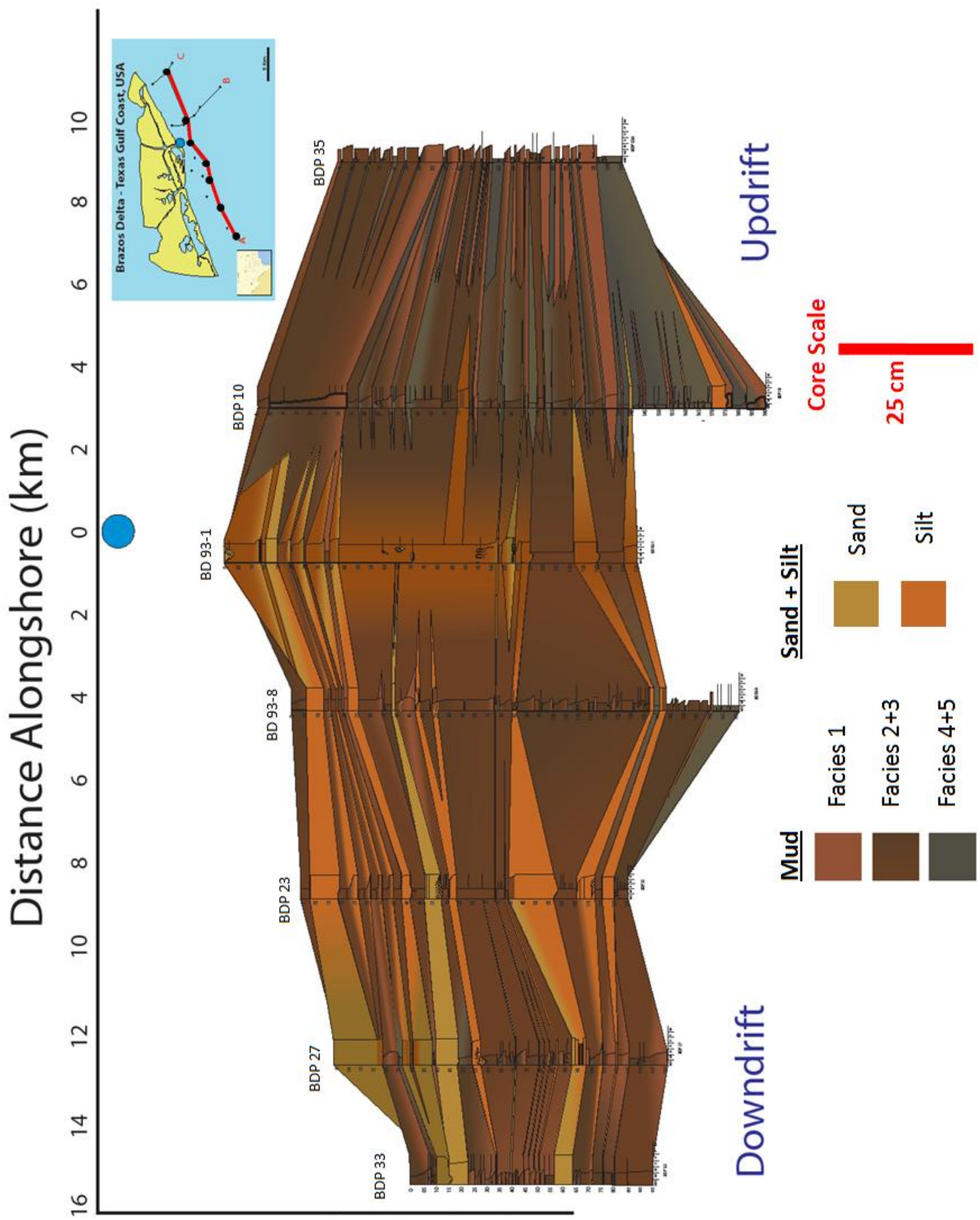


*Figure 15. Strike oriented cross section.*

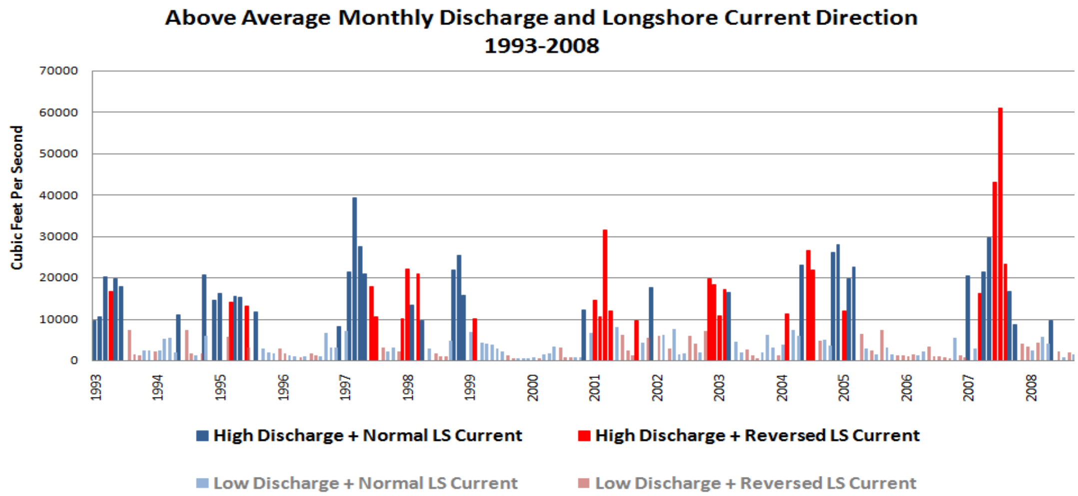


Normal Longshore Current: 36 Months
Reversed Longshore Current: 26 Months

*Figure 16. Comparison of discharge and longshore currents.*

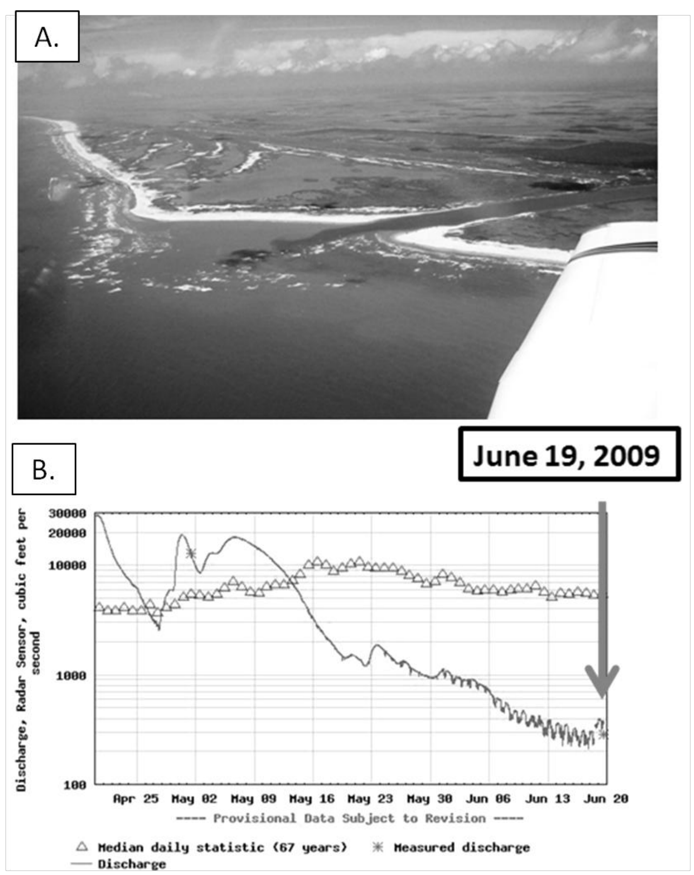


*Figure 17. A. Aerial photo taken on June 19th, 2009. B. Discharge of the Brazos River in 2009 through June.*

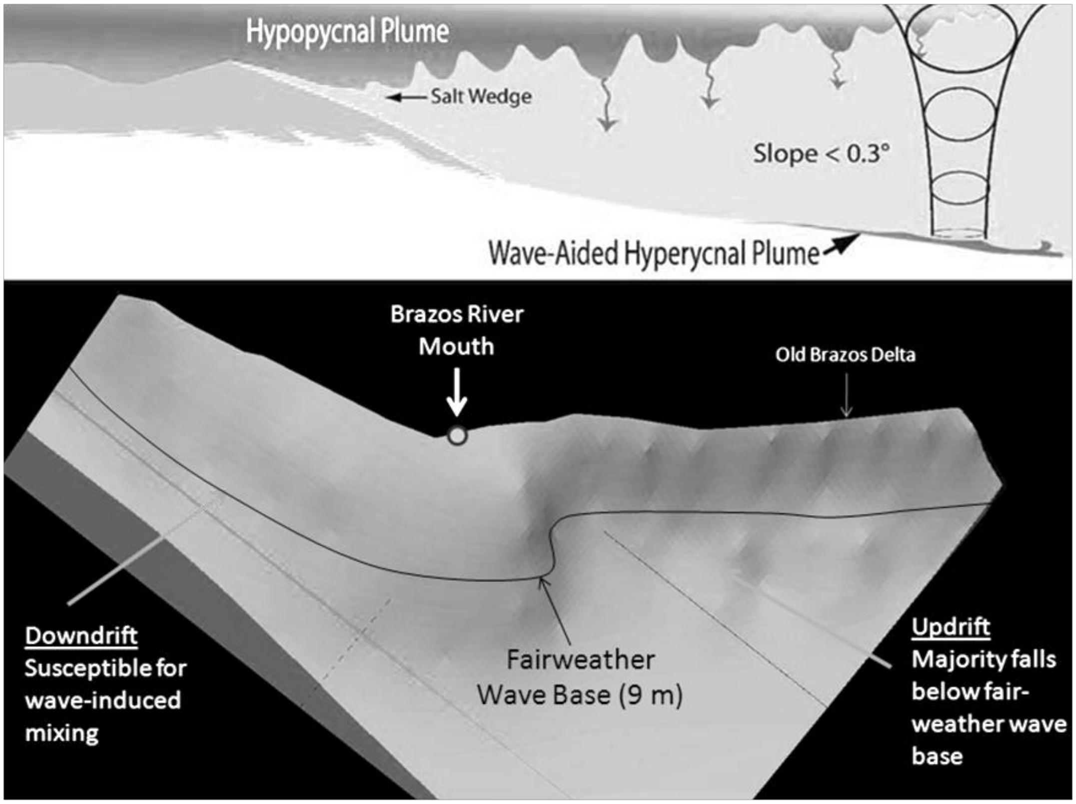


*Figure 18. A. Wave-aided hyperpycnal plume model. B. Bathymetry model of the Brazos Delta seafloor. From Rice et al., in review.*

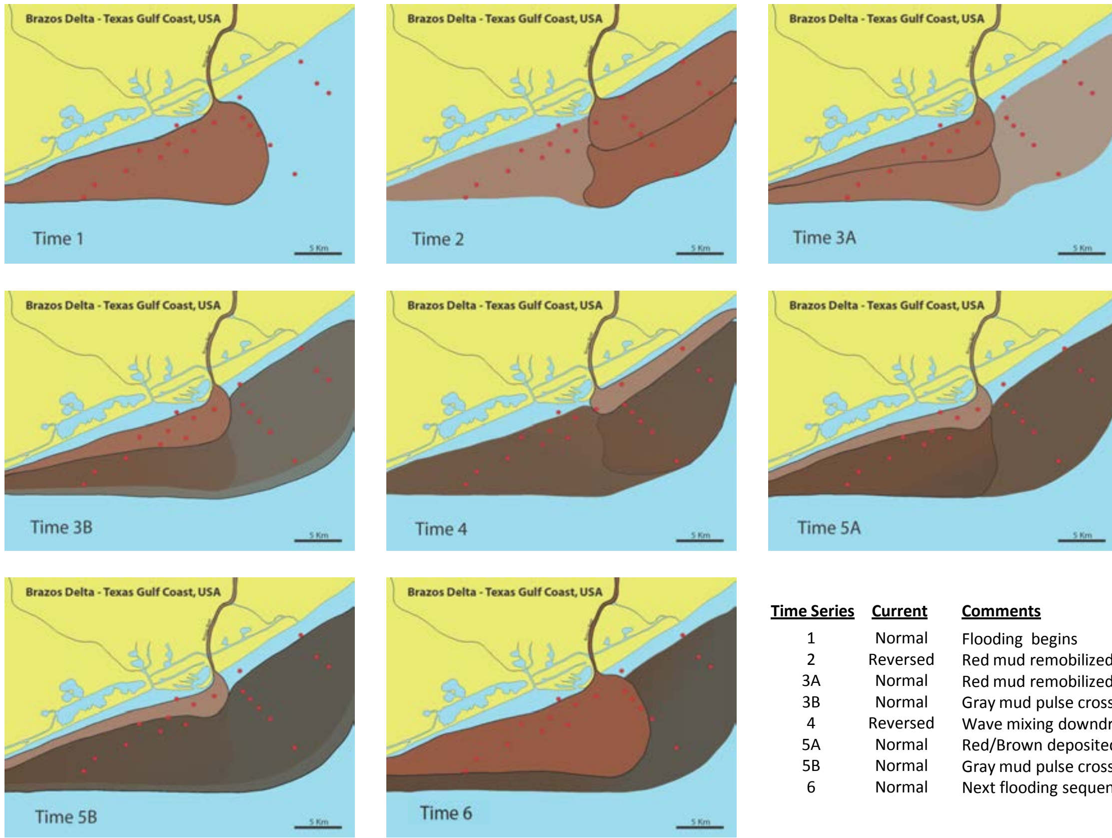


| Time Series | Current | Comments |
|---|---|---|
| 1 | Normal | Flooding begins |
| 2 | Reversed | Red mud remobilized updrift |
| 3A | Normal | Red mud remobilized downdrift |
| 3B | Normal | Gray mud pulse crosses delta |
| 4 | Reversed | Wave mixing downdrift |
| 5A | Normal | Red/Brown deposited downdrift |
| 5B | Normal | Gray mud pulse crosses delta |
| 6 | Normal | Next flooding sequence begins |

*Figure 19. Cartoon showing multiple possible stages in evolution of the facies observed in the modern Brazos Delta. Rice et al., in review.*

Key conclusions are:

1) In the Brazos prodelta and inner shelf, two end-member mud sources are identified, red-colored Brazos-river-derived sediment (kaolinite, illite, quartz, and calcite) and gray, Mississippi-derived mud (smectite, kaolinite, illite, and quartz). The two end member mud facies are far more abundant updrift, whereas mixed mud facies are the most common downdrift. This may be explained by the relative susceptibility of the downdrift muds to become mixed by waves, while the updrift mud facies are more stable. The abundance of gray Facies 4 mud updrift is likely due to its northeasterly source, while the downdrift region has far less gray mud because of the groin effects.

2) Downdrift mud packages have gradational transitions from red to brown to gray mud within mud packages, while updrift packages have sharp contacts between facies. The gradational contacts between mud facies downdrift are likely due to a quasi-constant supply of Brazos-derived sediment, due to the extended tail of the prodelta downdrift, as well as the effects of wave mixing. The sharp contacts updrift are likely due to a lesser susceptibility of wave-induced mixing, as well as a more pulsed supply of Brazos-derived sediment (during reversed currents) and longshore transport-derived gray muds (due to coastal storms).

3) Sand and silt beds are far more abundant downdrift than updrift, they typically occur within mud packages rather than at the base, and they are likely related to both normal suspension settling from floods, river-induced hyperpycnal flows, as well as high energy coastal storms.

4) The complex mixing of these two mud-sources suggests a dynamic and complex interaction of river-flood events, storm fronts, and wave-resuspension, with variable mixing of the two mud sources. Local changes in bathymetry, as well as river-groin effects also control the effectiveness of wave-resuspension and the degree of mixing.

5) The resulting prodelta muds show a distinct updrift- versus downdrift heterogeneity in porosity, permeability and potential preserved organic matter, which in turn has implications for the potential as an analog gas shale.

**Stop 3 – Old Brazos Delta at Surfside**

Lunch will be at this stop. See discussion above for Stop 2.

## Stop 4 – Follets Island

Follets Island is a small, ~2,500 year old barrier island located just west of Galveston Island. It is currently migrating landward at an average rate of just over 2 meters per year, making it one of the most vulnerable barriers along the Texas coast. Follets is a rollover barrier, as the rates of shoreline retreat equal the rates of landward bayline advance (Wallace et al., 2010). In order to put the current observations into a long-term context, sediment cores were collected over much of the island (Fig. 20) and radiometrically dated (Odezulu et al., in press). Sediment cores taken just offshore sampled a thin veneer (~3 m) of shoreface sand resting in sharp

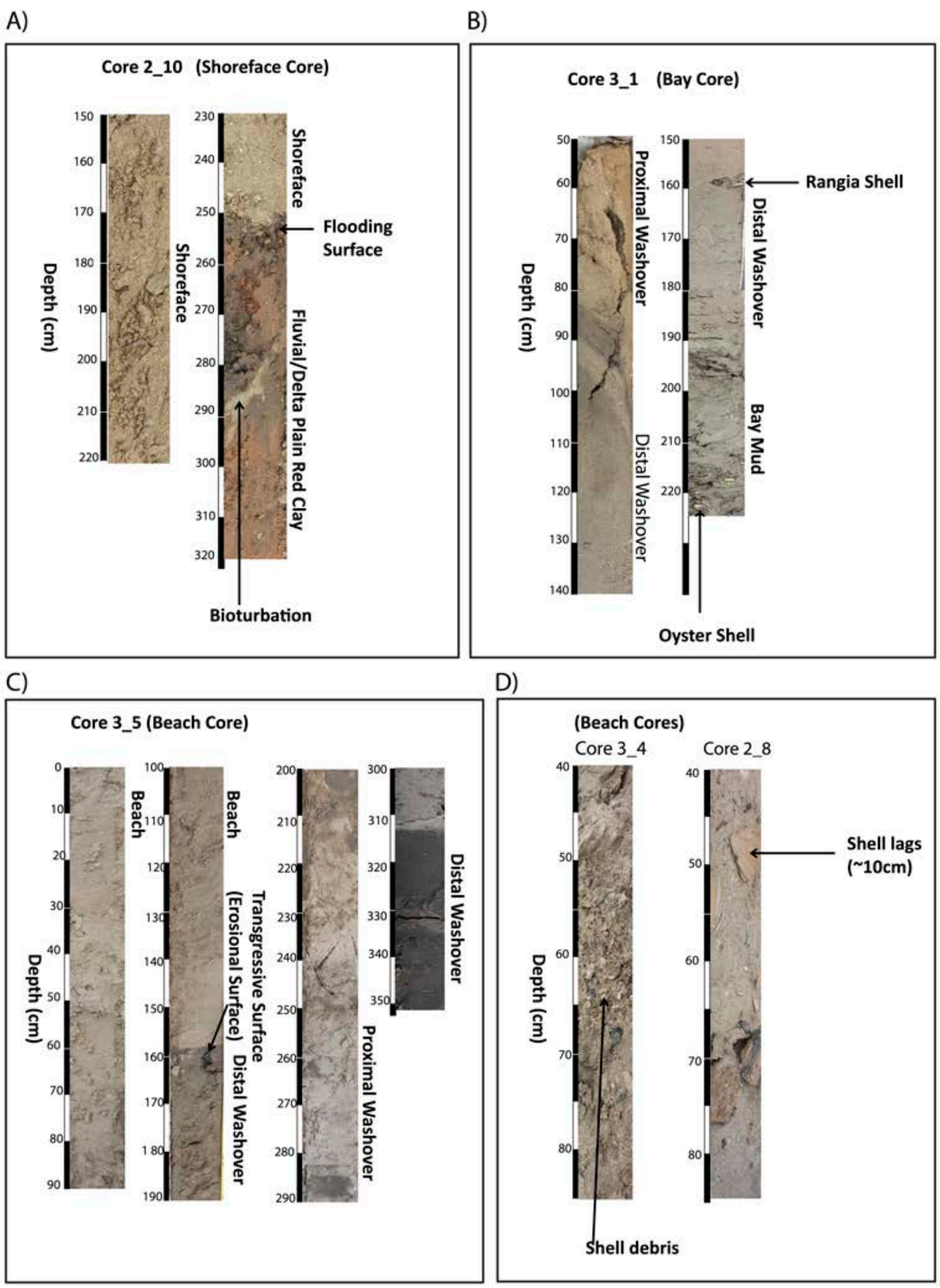


*Figure 20. Follets barrier subenvironment photographs (from Odezulu et al., in press). Note abrupt contacts between proximal and distal barrier deposits, indicating overall transgression.*

contact with ~3,000 year old Bastrop Channel fluvial/delta plain red clays. Cores from the bay sample proximal and distal washover resting in sharp contact with bay mud. Cores from the modern beach sample ~2 m of beach sand resting on distal and proximal washover. Figure 21 shows a cross section through the island constructed from all cores collected and dated. The stratigraphy confirms the rollover state of Follets Island over geologic time. Two flooding surfaces exist within the dataset, one deeper surface defined by the presence of marine deposits resting on fluvial deposits (yellow surface, Fig. 21) and a shallower surface defined by beach and upper shoreface deposits resting on distal washover and bay deposits (green surface, Fig. 21). Radiocarbon ages coupled with $^{210}Pb$ constrain short and long term rates of overwash. The long-term (last ~2,500 years) overwash flux for Follets Island is about 2,300 $m^3$/yr (~0.23 $m^3$/m/yr) (Wallace et al., 2010). The modern rate based on $^{210}Pb$ for the last ~80 years is ~15,200 $m^3$/yr (1.52 $m^3$/m/yr), meaning that the historical rate is about an order of magnitude faster.

These significant washover volumes are deposited into the bay, with about twice the volume as subaerial washover. Based on this sediment budget, overwash accounts for about half of what is eroded during shoreline erosional processes, and the rest of the deficit is moving southwest with the prevailing longshore currents. Due to this reduced sediment delivery coupled with accelerated sea level rise, Follets Island will transition from a subaerial barrier to subaqueous shoals (i.e., Chandeleur Islands) in a few centuries.

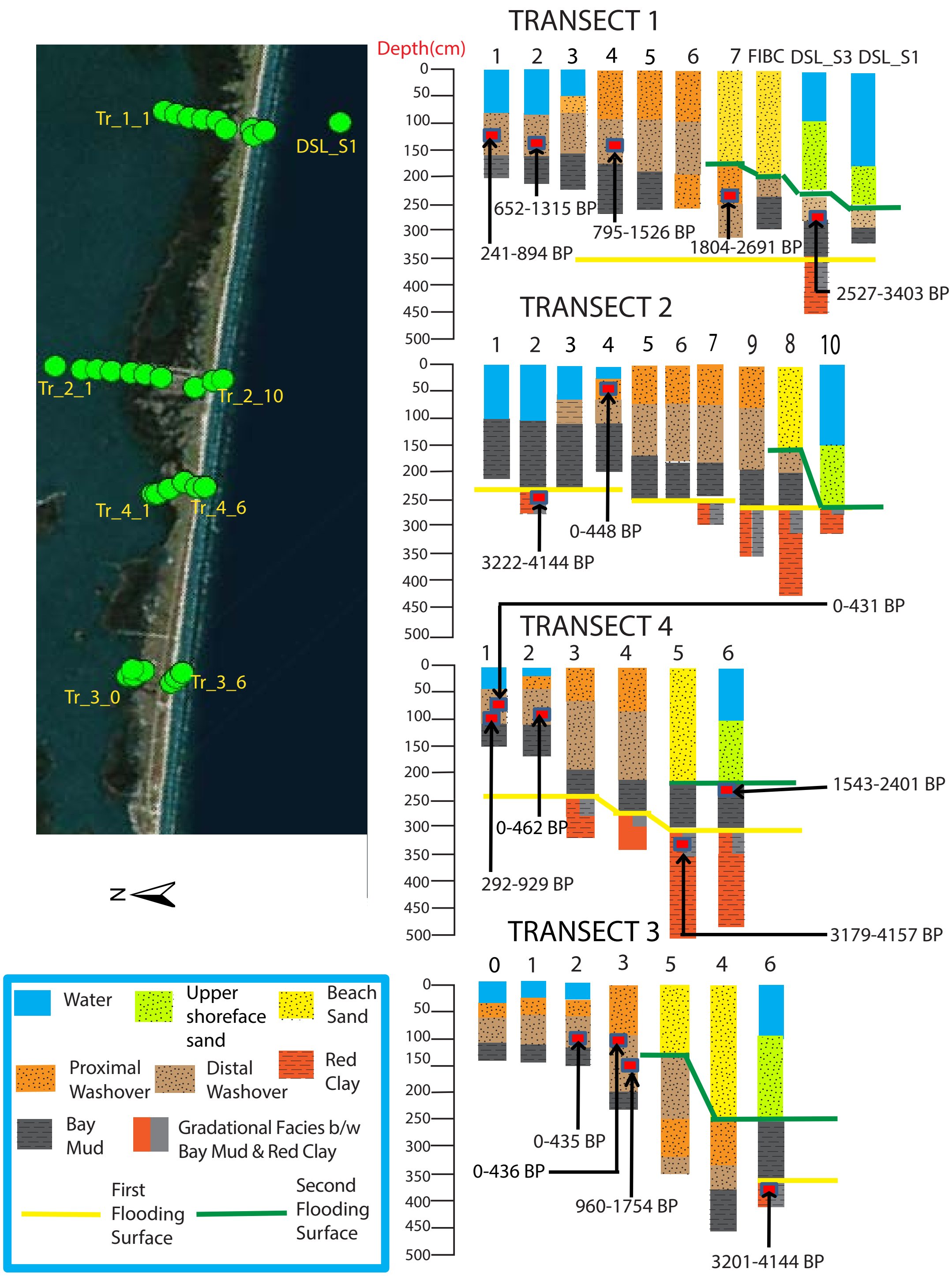


*Figure 21. Facies associated with core transects for Follets Island (from Odezulu et al, in press). Numbers with red squares are calibrated radiocarbon ages. Note a deeper (yellow line) and shallower (green line) transgressive surface.*

## Stop 5 - San Luis Tidal Inlet/Delta

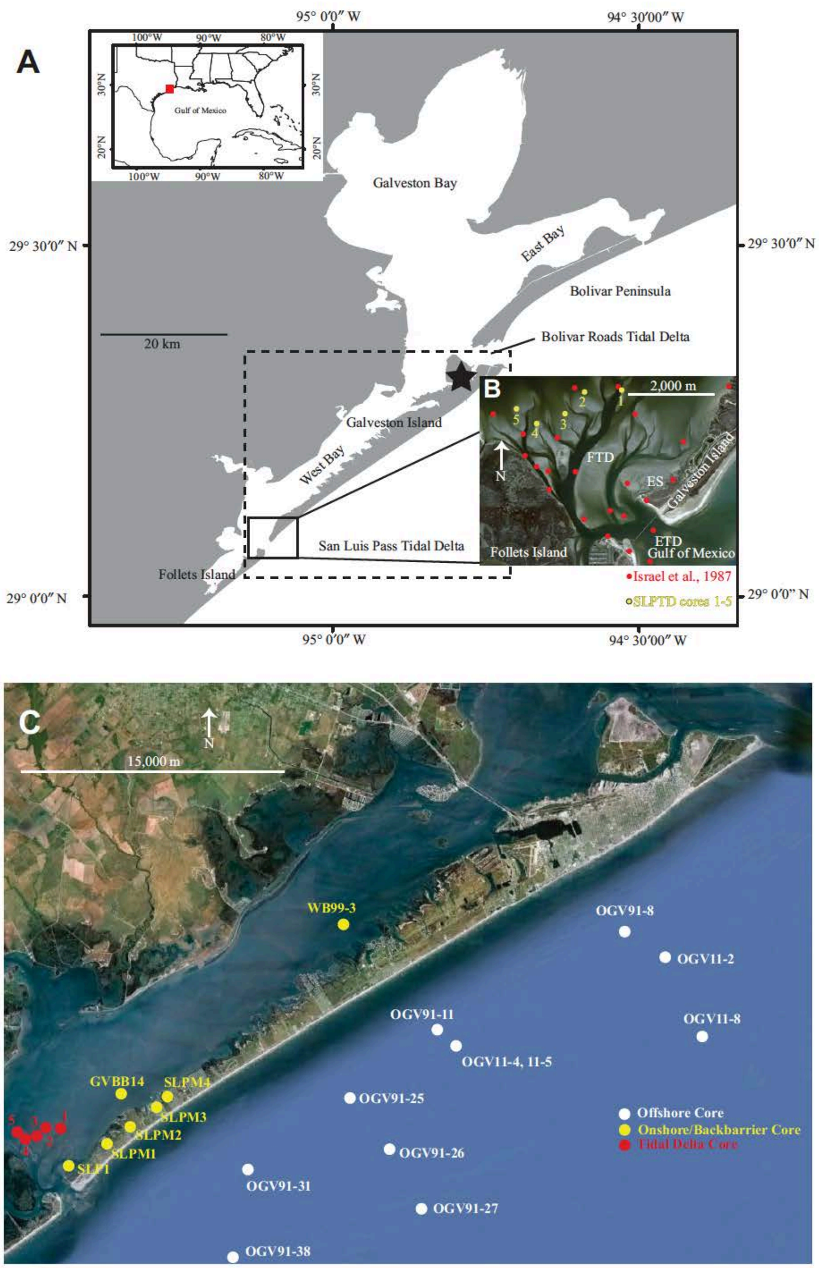


*Figure 22. (A) Study area. Dashed box shows location of (C). (B-C) Sediment cores used to examine the evolution of San Luis Pass and Galveston Island (from Wallace and Anderson, 2013).*

Because barrier islands are so extensive today, we tend to overestimate their contribution to the coastal stratigraphic record, certainly with regard to the transgressive systems track. In reality, landward and along strike migration of barriers and tidal inlets results in very extensive flood tidal deltas which, if deposited within incised fluvial valleys, have a much higher preservation potential than coastal barriers. This has certainly been the case on the east Texas shelf. During this field trip we will examine two flood tidal deltas, the San Luis and Bolivar flood tidal deltas.

San Luis Pass is a deep tidal inlet that separates Galveston Island from Follets Island (Fig. 22). It is incised into Pleistocene sediments to about -10 meters (Bernard et al., 1970; Williams et al., 1979; Israel et al., 1987). As we cross the bridge between Follets Island and Galveston Island, look to the right and you will see waves breaking over the San Luis ebb tidal delta. To your left you can see shallow tidal flats that comprise part of the flood tidal delta.

A detailed sedimentological analysis of the flood tidal delta was conducted by Israel et al. (1987). Their study showed that the tidal delta complex consists of a number of subenvironments including oyster reefs, washovers, distal tidal delta, proximal tidal delta, inlet, and marsh subenvironments.  The tidal inlet consists mainly of graded shell beds and shelly sands.  The aerial photograph of the delta (cover) shows the sandy lobes and tidal channels that comprise the proximal flood tidal delta.  Note that the flood tidal delta is significantly larger than the ebb tidal delta, which is under constant attack of large waves. By coupling the framework provided by Israel et al. (1987) with new radiometrically dated cores (Fig. 23), Wallace and Anderson, 2013 quantified detailed sand fluxes into San Luis Pass Tidal Delta (SLPTD) through time. The source of the sand into SLPTD is directly related to erosion from Galveston Island transported further southwest through longshore currents. From 200 to 2,100 years ago, the flux of sand into SLPTD was 4,700 $m^3$/yr, while the last 200 years (from historic maps coupled with sediment cores) yields a value of 10,000 $m^3$/yr. This more than doubling of the sand accumulation rate into SLPTD in historic relative to geologic time is directly related with erosion of Galveston associated with accelerated sea level rise punctuated by storms.

Sediment cores from the proximal portion of the delta sampled well-sorted sand and shelly sand and cores from the distal part of the delta sampled mostly mud with diagnostic thinly bedded sand/mud beds (tidal couplets) (Fig. 23).  Sedimentary structures are not

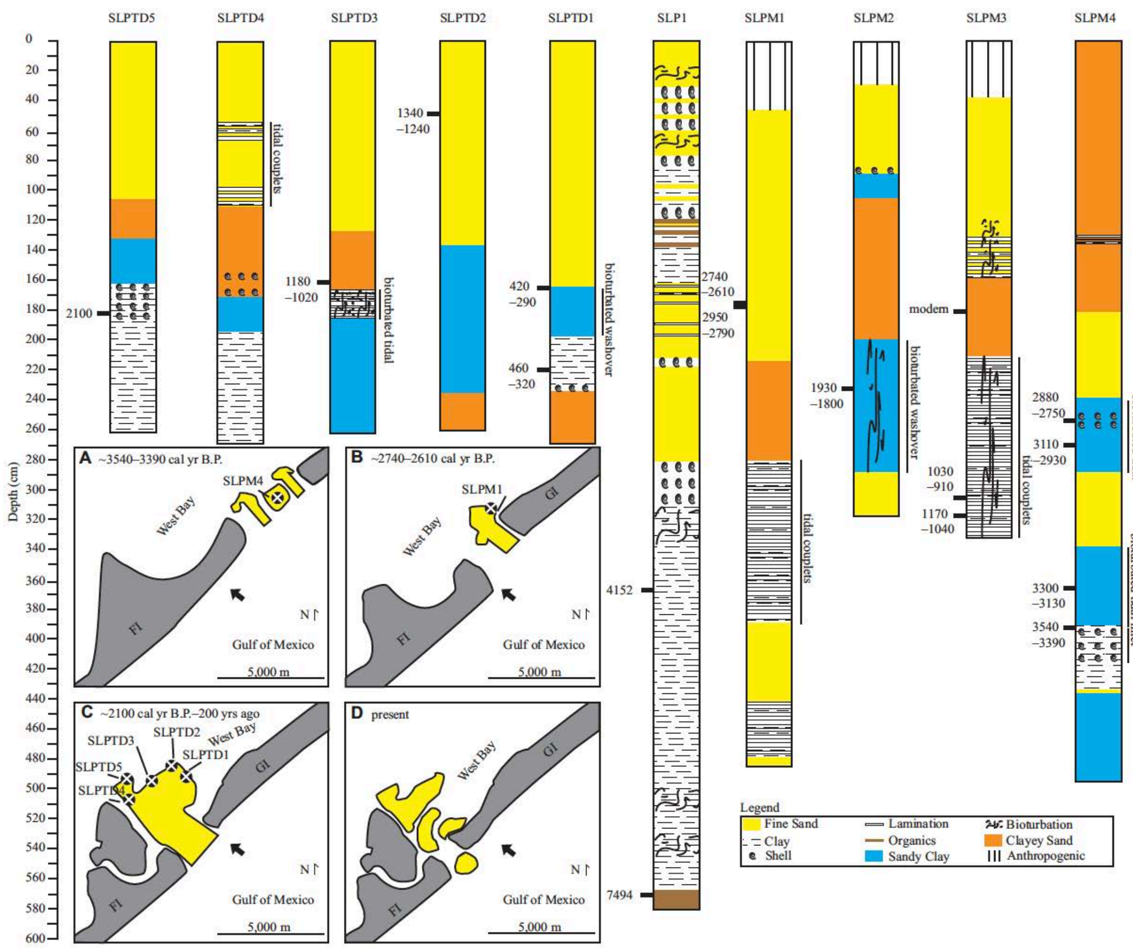


*Figure 23. Sediment cores used to examine the evolution of San Luis Pass Tidal Delta (SLPTD) (from Wallace and Anderson, 2013). (A-D) Evolutionary schematic showing coupled evolution of Galveston Is. (GI), SLPTD, and Follets Is. (FI).*

observed in cores from the proximal portion of the delta, but laterally shifting of tidal channels and sandy lobes occurs frequently and undoubtedly produces large-scale trough cross bedding and migration of large bedforms to create other large-scale structures. Both proximal and distal flood tidal delta facies interfinger with bay muds and organic-rich marsh deposits. Growth and development of the San Luis tidal inlet/delta complex was caused by westward accretion of Galveston Island over the last few millennia (Fig. 23). Around 2,100 years ago, westward migration of the inlet slowed when it reached an ancestral channel of the Brazos River, the Bastrop Channel. The inlet has now incised into the channel, and lateral accretion of the flood tidal delta has ceased and the flood tidal delta has prograded in a landward direction (Fig. 23).

Core SLP-91-1 (Fig. 23), taken at the backside of the western tip of Galveston Island, penetrated almost six meters of sediments. The cored interval consists of an overall coarsening upwards trend that reflects the westward migration of the tidal inlet, flood tidal delta and barrier island and infilling of the Bastrop Channel fluvial channel. A highly cohesive, organic-rich, olive-black clay interpreted as a freshwater marsh deposit underlies the sequence. A radiocarbon age date of 7,500 ± 75 cal BP was acquired from this organic-rich sediment. This is overlain by dark greenish gray bioturbated clay unit, interpreted as bay/estuarine sediments, grading up to brown to reddish brown clay unit, interpreted as a prodelta deposit of the Brazos River. The upper clay unit is moderately bioturbated and contains unarticulated *Crassostrea* shells. The Brazos River clay unit is overlain by stacked fine sands and clay laminations with shell lag bases, interpreted as flood-tidal deposits.

A radiocarbon age date of 4,150 ±191 cal BP was obtained from an articulated *Cyrtopleura costata* (Angel Wing) shell sampled at the base of the flood-tidal delta deposits, in the Brazos river clay unit. This bivalve is indicative of tidal inlet areas, and may burrow up to 0.5 m into clay substrate. This unit is capped by a coarsening upward sequence of bay/lagoon clay with sand and shelly sand laminations and interbeds with abundant plant debris, interpreted as washover deposits. These deposits grade up into stacked graded shell lag to fine sand beds representing the shallowing upwards and emergence of the flood-tidal delta.

## Stop 6 - Galveston Island

Barrier islands and peninsulas are common features of modern low-gradient coasts. They are considered transgressive features. Galveston Island (Fig. 24) is one of the best-studied barrier islands in the world and its evolution is well established. The island began to form about 5,500 years ago and, for most of its history it grew and advanced seaward. The growth of the island left an imprint of the landscape that is seen in aerial photographs, similar to coastal landscapes along many of the shorelines of the world (Fig. 25). This landscape consists of linear ridges and swells between these ridges. The ridges are the highest natural features on the island and the swells provide most of the islands limited freshwater habitats.


*Figure 24. Satellite image showing extent of Galveston Island.*

Borings through the island and radiometric age dating detail the evolution of the island (Bernard et al., 1970). This and more recent work (Rodriguez et al., 2004) showed that the island prograded seaward during the past 5,000 years, when the rate of sea-level rise slowed. Figure 26 shows the Pleistocene-Holocene boundary forming a ramp that shallows to a depth of -3 m on the landward side of the island. This ramp served as a nucleus for growth of the island. Bernard and his colleagues interpreted the island as having formed from a small bar that emerged and grew seaward by beach accretion and southwestward by spit accretion (Bernard et al., 1970). The geometry of the beach ridges at the backside of the northeastern half of the island defines a set of ridges that fan-out towards the bay. This indicates that, initially, the island grew northeastward towards the bay, similar to a spit bar, using the shallow portions of the Pleistocene-Holocene surface as an anchor. The ridges later rotated out towards the Gulf. Storm surge channels dissect older beach ridges and mark episodes when the younger, narrower barrier was breached.

The radiocarbon dates obtained by Rodriguez et al (2004) were acquired largely from monospecific samples, mostly *Donax* shells. This species lives only in the intertidal swash zone. In general, the newer data support the Bernard et al. (1970) results, indicating that the progradation of the island took place between approximately 5,300 years ago and 1,200 years ago, based on the age of the most seaward shoreface deposits. After this time, the island began its landward retreat.

What is the origin of the sand that now comprises Galveston Island? Detailed mineralogical analyses by Cole and Anderson (1982) showed that the island is made up of sand derived from the Mississippi, Trinity/Sabine, and Brazos rivers, in almost equal proportions.

Currently, the only sand that exists offshore of the shoreface occurs within the Trinity/Sabine incised fluvial valley. Thus, transgressive erosion has been highly efficient at transporting sand onshore to nourish barriers. These sands were stacked in shingle-like fashion against a Pleistocene surface whose profile mimics the modern shoreface profile (Fig. 26). Ridge and swell topography marks the episode of barrier growth (Fig. 25). A higher sediment supply during the early phase of relative stillstand, provided by reworking of previous coastal lithosomes, hastened spit progradation and seaward accretion of barriers. When the offshore sand supply was exhausted, the barrier began to erode. The modern beach is an erosional surface cut into beach ridges that range in age from several centuries old to nearly 2,000 years old.

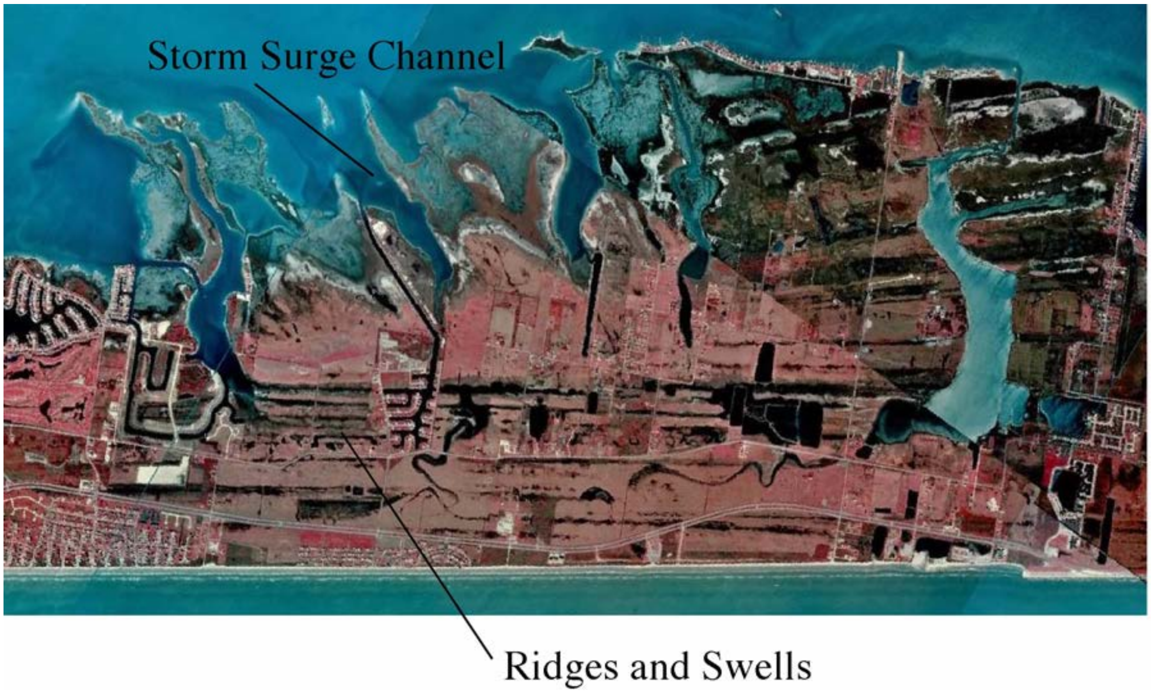


*Figure 25. Ridge and swell topography of Galveston Island.*

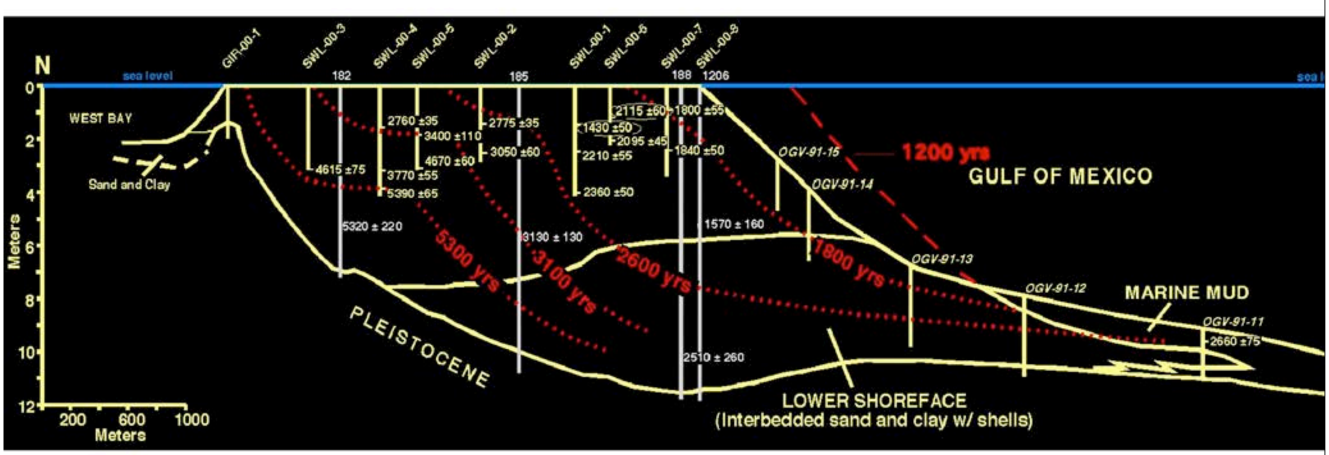


*Figure 26. Geological cross section through Galveston Island based on the combined results of Bernard et al. (1970) and Rodriguez et al. (2004).*

The relief on the Pleistocene surface, which is mainly related to the Trinity incised fluvial valley, mainly controls the thickness variations. Recall that fluvial terraces formed during the falling stage of sea level characterize the valley. For the most part, the sands that fill the flanks of the valley and interfluvial areas are less than 8 meters thick. Thus, these portions of the barriers would not survive transgressive erosion. The only coastal deposits that would be preserved are those that fill the deeper portions of the Trinity/Sabine incised valley (Fig. 1). Indeed, the only ancient coastal lithosomes to have escaped transgressive erosion during the past are those that occur within the valley. The continental shelf offshore of Galveston Island is virtually barren of sand, the only exception being transgressive sand banks and tidal and fluvial sands that occur in the Trinity/ Sabine incised fluvial valley. We will discuss these later.

Coring transects offshore of Bolivar Peninsula and Galveston Island have shown that the present toe of the shoreface occurs at an average depth of 8 meters; it is marked by a change in gradient and the seaward limit of shoreface-attached sand bodies. The Holocene ravinement surface, mapped by Siringan and Anderson (1994), eroded to depths between -5 to -8 m and is generally a planar surface, although scarps or step-like features do occur and probably result from changes in the rate of sea-level rise and associated shoreline retreat. The ravinement surface generally coincides with the Holocene-Pleistocene unconformity. In cores, a sharp increase in stiffness and cohesiveness, low water content, the occurrence of calcareous nodules, and indications of oxidation (color ranges from red, brown, yellow, gray, to tan), occurs across the Holocene-Pleistocene boundary.

Sediment cores from the continental shelf sampled a thin (less than one meter thick) unit of marine mud resting directly on the ravinement surface. Event storm beds, while thin (Siringan and Anderson, 1994), were recently quantified as permanent sand lost from the island below storm wave base (Wallace and Anderson, 2013). The rates of storm erosion offshore are indeed limited, and therefore attest to the great efficiency of shoreface ravinement in forcing onshore transport of sand during transgression.

**Coastal Erosion**

All along the coast we will observe signs of beach erosion (Fig. 27). The average rate of erosion for the upper Texas coast is 3 to 5 feet per year. As geologists, we know that this transgression has been going on for thousands of years. In fact, the rate of shoreline retreat is significantly slower now than it was a few thousand years ago. Try to tell this to the people who own houses on the beach; they are convinced that erosion is a recent phenomenon and somebody is to blame. The sad part is that if predictions about increased sea-level rise in the next century prove accurate, the rate will increase.

When it comes to beach erosion, Texans have two options: 1) allow the beaches to erode, or 2) nourish the beaches with sand. Current state law requires that as the beach advances landward and overtakes private property, the property owner must remove their house at their own expense. This is called the right to access law, meaning that all citizens must have free access to the beaches. Many property owners think that this law is unfair and that they have a right to protect their property, even if that necessitates constructing seawalls and other hard structures.

*Figure 27. This photograph shows one of the few remaining seawalls on the upper Texas coast at Surfside. Note that the beach is virtually gone and the elevation of the beach has been lowered by about 4 ft since the wall was constructed.*

Recent efforts on the part of beach-front property owners to save their property have included the construction of straw dunes and Geotubes. The latter are large tubes of fiberglass fabric filled with sand. The straw dunes lasted only until the first small tropical storm and the Geotubes are being undercut by waves in several locations. Where they still stand, the beach is becoming narrower, which will eventually result in a lack of access to the beach, a violation of Texas Law.

What happens to the area offshore of the beach as the shoreline retreats landward? The answer is that the shoreface retreats landward at about the same rate. This is how the transgressive ravinement surface is created. Coastal geologists have a reasonably good understanding of the process of shoreface retreat and there are several models that illustrate how the processes occur.

Many property owners feel that beach nourishment is the answer to their problems. But, this is a losing battle - the sand is placed in a setting where wave reworking eventually will remove it from the beach and deliver it to the deeper water environment or farther along shore. It is interesting to note that the continental shelf offshore of Galveston Island is virtually barren of large, concentrated sand deposits, with the exception of small concentrated sand banks deposited along the margins of the Trinity/Sabine incised fluvial valley during an earlier phase of sea-level rise. In short, there are no offshore sand resources available for beach nourishment and re-supplying the beaches is a short-term solution. The reality is, if Texans truly want to have free access to their beaches, we will need codes the prohibit construction within one hundred meters of the beach.

The wetlands behind the barrier systems are valuable and protected areas. Where sand is not available to the barrier system, the dunes are not developed, the beach is narrow, and the roads wash out. Rebuilding of the highways often is not an available option. The advancing sea in about a decade will overrun the road we are driving on, unless a major storm destroys it first. Note how much property is for sell along the highway.

**Stop 7 - The Galveston Seawall and the 1900 Storm**

Around the turn of the century, Galveston was a thriving port city with a population of almost 38,000. Too a large degree, the prosperity of Galveston at this time can be attributed to the deep tidal channel that served as a ship channel for deep draft vessels. On September 8, 1900 the deadliest natural disaster in the history of the United States struck the island. A storm with winds over 190 kilometers per hour (120 miles per hour) and an overwhelming tidal surge decimated the island and killed over 6,000 people. One-third of the city was completely destroyed (Fig. 28).

In response to the devastating event, the city built a seawall 11 kilometers long and 5 meters high. The wall is 1 to 2 meters wide at the top and expands to 5 to 6 meters wide at the base. Accompanying the building of the seawall, the city raised the level of part of the island by 1 to 2 meters (Fig. 29). When the Galveston seawall was complete in 1910, the beach was ~30 meters seaward of the present coastline. During the early 1900s the city continued to prosper. As we drive through the older part of the city you will see many of the beautiful Victorian houses that were constructed during this era.

*Figure 28. Galveston in the aftermath of the 1900 storm.*

*Figure 29. The raising of Galveston Island.*

Ironically, it was not the 1900 hurricane, but the construction of the Houston Ship Channel that led to the economic downfall of Galveston during the depression and post-World War II era. Galveston suffered while Houston grew. In recent years Galveston's economy has been re-energized by tourism. But, now the city faces another problem. Its beaches are eroding at a rate of more than a meter per year. An attempt to nourish the beaches met with only modest success and there is a serious shortage of sand needed for future nourishment projects. In the end, Galveston will probably loose its battle with nature. The retreat of the island can best be seen where the seawall ends; a dramatic break occurs between the seaward anchored seawall and the more landward placement of the natural beach.

## Acknowledgments

This field guide was modified from guides developed by Dr. John Anderson and his students at Rice University, Houston, Texas, and is based extensively on their work. Appreciation is extended to Dr. Anderson and his previous students, including, Dr. Stephanie Shipp, Dr. Patrick Taha, Dr. Alex Simms, Dr. Antonio Rodriguez, Dr. Fernando Siringan. Dr. Ken Abdulah, Mr. Michael Hamilton, Dr. Mark Thomas, and Dr. Louis Bartek as well as to Dr. Alison Henning who developed this guide for use with teachers.

## References

Anderson, J.B., Wallace, D.J., Simms, A.R., Rodriguez, A.B., Weight, R.W., and Taha, Z.P., 2016, Recycling Sediments Between Source and Sink During a Eustatic

Cycle: Systems of Late Quaternary Northwestern Gulf of Mexico Basin: Earth-Science Reviews, v. 153, p. 111-138.
Bernard, H.A., Major, C.F., Parrott, B.S., and LeBlanc, R.J., 1970, Recent Sediments of Southeast Texas: a Field Guide to the Brazos Alluvial and Deltaic Plains and the Galveston Barrier Island Complex: Univ. of Texas at Austin, BEG, Guidebook 11, 132 p.
Cole, M.L., and Anderson, J.B., 1982, Detailed grain size and heavy mineralogy of sands of the northeastern Texas Gulf coast: implications with regard to coastal barrier development: Trans. Gulf Coast Geol. Socs., v. 32, p. 555-563.
Fracticelli, C.M., 2006, Climate Forcing in a Wave-Dominated Delta: The Effects on Drought-flood Cycles on Delta Progradation, Society of Sedimentary Geology, v. 76, p.1067-1076.
Israel, A.M., Ethridge, F.G., and Estes, E.L., 1987, A sedi- mentologic description of a micro-tidal, flood-tidal delta, San Luis Pass, Texas: Journal of Sedimentary Petrology, v. 47, p. 288–300.
Mulder, T., Syvitski, J.P.M., Migeon, S., Faugeres, J.-C., Savoye, B., 2003, Marine hyperpycnal flows: initiation, behavior and related deposits. A review: Marine and Petroleum Geology, v. 20, p. 861-882.
Odezulu, C.I., Lorenzo-Trueba, J., Wallace, D.J., and Anderson, J.B., *in press*, Follets Island: a case of unprecedented change and transition from rollover to subaqueous shoals, in Moore, L. and Murray, B., eds., Barrier Dynamics and the Impacts of Climate Change on Barrier Evolution, Springer Science + Business Media Dordrecht.
Rice, D., Wellner, J.S., Bhattacharya, J., and Dellapenna, T., in review, Major Changes Over Minor Distances: An Offshore Micro-Stratigraphic Study of the Modern Asymmetric Wave-Influenced Brazos Delta, Texas Gulf Coast USA, Journal of Sedimentary Research.
Rodriguez, A.B., Hamilton, M.D., and Anderson, J.B., 2000, Facies and evolution of the modern Brazos delta, Texas: wave versus flood influence: Journal Sedimentary Research, v. 70, p. 283-295.
Rodriguez, A.B., Anderson, J.B., Siringan, F.P., and Taviani, M., 2004, Holocene evolution of the east Texas coast and inner continental shelf: along-strike variability in coastal retreat rates, Journal of Sedimentary Research, v. 74, p. 406-422.
Siringan, F.P. and Anderson, J.B., 1994, Modern shoreface and inner-shelf storm deposits off the east Texas coast, Gulf of Mexico: Journal Sedimentary Research, v. B64, p. 99-110.
Taha P.Z., Anderson J.B., 2008, The Influence of Valley and Listric Normal Faulting on Styles of River Avulsion: A Case Study of the Brazos River, Texas, USA, Geomorphology, 95, Pages 429-448.
Wallace, D.J., and Anderson, J.B., 2013, Unprecedented erosion of the upper Texas Coast: Response to accelerated sea-level rise and hurricane impacts: Geological Society of America Bulletin, v. 125, no. 5-6, p. 728-740.
Wallace, D.J., Anderson, J.B., and Fernández, R. A., 2010, Transgressive ravinement versus depth of closure: A geological perspective from the upper Texas coast: Journal of Coastal Research, v. 26, no. 6, p. 1057-1067.

Williams, S.J., Prins, D.A., Meisburger, E.P., 1979. Sediment distribution, sand resources and geologic character of the inner continental shelf off Galveston County, Texas. United States Army Corps of Engineers, Miscellaneous Report 79-4, 159 pp.